



Title	Contribution of Microstructures and Compositions to the Mechanical Properties of Human Dentin
Author(s)	武田, 侑子
Citation	大阪大学, 2014, 博士論文
Version Type	VoR
URL	https://doi.org/10.18910/34352
rights	
Note	

The University of Osaka Institutional Knowledge Archive : OUKA

<https://ir.library.osaka-u.ac.jp/>

The University of Osaka

**Contribution of Microstructures and Compositions
to the Mechanical Properties of Human Dentin**

象牙質の微細構造および組成が機械的強度に及ぼす影響

**Osaka University Graduate School of Dentistry
Department of Restorative Dentistry and Endodontology
Supervisor: Professor Mikako Hayashi**

Yuko Takeda

ACKNOWLEDGEMENTS

I would like to express my sincere gratitude to my supervisor, Professor Mikako Hayashi, Head of the Department of Restorative Dentistry and Endodontology at Osaka University Graduate School of Dentistry, a tender-hearted teacher, for countless discussions and valuable advice, as well as her patience and constant support throughout the years.

I am also very much thankful to Professor Takayoshi Nakano, Head of the Division of Materials and Manufacturing Science at Osaka University Graduate School of Engineering, for providing me valuable advice and a lot of support. I am deeply grateful to Dr. Takuya Ishimoto, Osaka University Graduate School of Engineering, for technical helps and useful discussions.

I greatly appreciate Dr. Mitsuru Saito, Department of Orthopaedic Surgery, The Jikei University School of Medicine, for his tremendous support for the collagen analysis.

Many thanks also go to all members of the Department of Restorative Dentistry and Endodontology for spending valuable time helping me.

Yuko Takeda
February 2014

INDEX

INTRODUCTION	1
Chapter 1: Mechanical strength of human dentin in relation to individual differences in microstructures and its compositions at the visible level	
1.1 Materials and methods	4
1.1.1 Preparation of dentin specimens	
1.1.2 Measurement of mineral density	
1.1.3 Measurement of flexure strength and fracture toughness	
1.1.4 Calculation of dentinal tubule density and degree of occluded tubule lumens	
1.1.5 Measurement of hardness and Young's modulus	
1.2 Results	7
1.2.1 Mineral density	
1.2.2 Flexure strength and fracture toughness	
1.2.3 Dentinal tubule density and degree of occluded tubule lumens	
1.2.4 Hardness and Young's modulus	
1.3 Discussion	9
1.4 Conclusion	12
Chapter 2: Mechanical strength of human dentin in relation to individual differences in microstructures and its compositions at the molecular level	
2.1 Materials and methods	14
2.1.1 Preparation of dentin specimens	
2.1.2 Analysis of apatite orientation	
2.1.3 Measurement of collagen/mineral ratio	
2.1.4 Quantification of advanced glycation end-products (AGEs)	
2.2 Results	16
2.1.1 Apatite orientation	
2.1.2 Collagen/mineral ratio	
2.1.3 AGEs content	
2.3 Discussion	17
2.4 Conclusion	19

Chapter 3: Dominant factors to mechanical strength of human dentin	
3.1 Materials and methods	20
3.2 Results	20
3.3 Discussion	21
3.4 Conclusion	21
GENERAL CONCLUSIONS	22
REFERENCES	23
TABLES AND FIGURES	

INTRODUCTION

Dentin is a hard tissue that constitutes the majority of human teeth. It is comprised of approximately 70w% of inorganic material, 20w% of organic material, and 10w% of water, which correspond to 45, 33, and 22v%, respectively¹⁾. Dentin mostly consists of type I collagen and hydroxyapatite^{1, 2)}. Microstructural features of dentin are dentinal tubules, peritubular, and intertubular dentin. Dentinal tubule with internal diameters of approximately 1 μm is oriented radially from the pulp toward the dentin-enamel junction. Each tubule is surrounded with a highly mineralized cuff named peritubular dentin^{1, 3)}. Intertubular dentin occupies the internal space between the peritubular cuffs and consists of mineralized collagen fibrils arranged in a felt-like structure oriented perpendicular to the tubules⁴⁾. Tubule density increases towards the pulp due to the convergence of tubules and doubling of tubule diameters¹⁾.

Individual differences in the microstructures and compositions of dentin have been considered to affect the mechanical strength of teeth. Therefore, the mechanical strength of human dentin has been investigated from various structural and environmental aspects. For instance, it was reported that flexure strength of aged dentin ($50 \leq \text{age} \leq 80$) was significantly lower than that of young dentin ($17 \leq \text{age} \leq 30$)⁵⁾. Dentin is known to alter its form to transparent (or sclerotic) dentin with aging because the tubule lumens gradually filled with mineral^{1, 6-8)}. This alteration usually begins at the apical end of the root and often extends into the coronal dentin^{1, 9)}. Webber *et al.*¹⁰⁾ claimed that up to 50% of the dentinal tubules can become completely occluded with age under natural physiological conditions. Accordingly, mineral density in transparent root dentin was significantly higher than that of normal dentin and its fracture toughness was 20% lower than that of normal root dentin¹¹⁾. However, it is not clear whether occluded tubule lumens alone or any other alterations in intertubular dentin are responsible for the low fracture strength of aged dentin¹²⁻¹⁵⁾.

Dehydration has been investigated as an influential environmental factor that significantly affects the strength of dentin. It was found that dentin with age over 50 years contained less water than young dentin (10–20 years of age)¹⁶⁾. This may be because water permeability of dentin decreased with the reduction in tubule diameter due to occlusion with aging¹⁷⁾. Dehydrated dentin showed less strain at fracture than hydrated dentin and demonstrated its brittle behavior¹⁸⁾. Fracture toughness of dehydrated dentin was also significantly lower than that of hydrated dentin¹⁹⁾. Moreover, the fatigue crack growth rate of the young hydrated dentin was significantly lower than that of the hydrated old and dehydrated young dentin²⁰⁾.

Tubule orientation has also been known as an important factor that influences the mechanical properties of dentin^{21–27)}. Flexure and tensile strengths of dentin showed anisotropy in terms of dentinal tubule orientations. Dentin with tubule orientation perpendicular to their long axis and short axis of a beam-shaped specimen had significantly higher flexure and tensile strengths than that with tubule orientation parallel to their long axis^{21–25)}. Furthermore, the mechanical properties of dentin associated with its tubule density have also been investigated^{21, 22)}. Dentinal tubule density in an enamel side (11,000–30,000 tubules/mm²) was significantly lower than that in a pulp side (50,000–70,000 tubules/mm²), and the flexure and tensile strength of dentin in the enamel side were significantly higher than those in the pulp side.

Miguez *et al.*²⁸⁾ demonstrated the significant contributions of collagen to the mechanical properties of dentin. The contents of two major enzymatic cross-links (dihydroxylysinonorleucine and pyridinoline) in root dentin were significantly higher than those in crown dentin, and the authors explained that this contributed to the higher tensile strength of root dentin compared with that of crown dentin. Açıl *et al.*²⁹⁾ examined the contents of deoxypyridinoline and pyridinoline in dentin in relation to aging and showed that both cross-links did not increase with aging. Non-enzymatic cross-links known as advanced glycation end-products (AGEs) have also been

investigated. Miura *et al.*³⁰⁾ confirmed by immunohistochemical analysis that *N*-carboxymethyllysine (CML), which is one of the AGEs, accumulated in dentin collagen with aging.

However, all these studies presented the mechanical properties of dentin in relation only to a few factors and very few studies analysed multiple factors by using the same tooth. Therefore, the elements that dominantly affect the mechanical properties of dentin have not been fully understood.

Bone is a hard tissue and has similar composition to dentin^{1, 2)}. Bone mineral density (BMD) is correlated with bone strength³¹⁾. However, the National Institutes of health (NIH) consensus statement about osteoporosis presented that bone mineral density is not an absolute parameter accounting for all of bone mechanical properties, but bone strength should be determined by two features—bone density and bone quality³²⁾. Bone density is expressed as grams of mineral per area or volume, while bone quality refers to architecture, turnover, and damage accumulation such as microfractures and mineralization. Bone density is frequently used as a proxy measure and accounts for approximately 70% of bone strength. The remaining 30% accounts for bone quality. Recently, bone strength has been evaluated in terms of both structural and quality parameters^{33, 34)}. Structural parameters include microstructures such as cancellous bone trabeculae and porosity of the cortical bone, while quality parameters consist of mineralization, mineral orientation, collagen cross-links, and microcracks. Since most of the parameters of bone are in common with those of dentin, the same evaluation methods in bone strength might be applied for assessing dentin strength.

The purposes of this study were to investigate the individual differences in microstructures and compositions of human dentin in terms of structural and quality parameters, and to identify the dominant factors that most contributed to its mechanical strength.

Chapter 1

Mechanical strength of human dentin in relation to individual differences in microstructures and its compositions at the visible level

1.1 Materials and methods

1.1.1 Preparation of dentin specimens

Freshly extracted human molars ($n = 46$), whose origin and background including age, gender, type of tooth, and reasons for extraction could be identified and which were free of fractures and caries, were stored in Hanks' balanced salt solution (HBSS) at 4°C and used within 3 months since extraction. The protocols used were approved by the ethics committee of Osaka University (H21-E29). Beam-shaped specimens of crown dentin with three different dentinal tubule orientations, which measured approximately $1.7 \times 0.2 \times 8.0$ mm, were sectioned by a low-speed diamond saw (ISOMET2000, Buehler) and adjusted with an emery paper (#1500, Buehler) with a polisher (ECOMET III, Buehler). The three tubule orientations were as follows (Fig. 1A): transverse was regulated by the tubule orientation parallel to the long axis of the specimen, in-plane longitudinal was regulated by the tubule orientation perpendicular to the long axis and parallel to the short axis of the specimen, and anti-plane longitudinal was regulated by the tubule orientation perpendicular to the long axis and short axis of specimen. A root specimen measuring approximately $1.2 \times 0.2 \times 5.0$ mm was also regulated by the long axis of the specimen parallel to the tooth axis (Fig. 1A). The three crown and one root specimens were obtained from one tooth. Semicircle-shaped specimens of crown dentin, sectioned parallel to the tooth axis with a thickness of approximately 0.8 mm, were also obtained from the same tooth (Fig. 1B).

1.1.2 Measurement of mineral density

Beam-shaped specimens of crown and root dentin were scanned with a peripheral quantitative computed tomography (CT; XCT Research SA, Stratec Medizintechnik). The specimens were kept fully hydrated in acrylic tubes during scanning. Each specimen was scanned at three locations longitudinally with intervals of 0.4 mm in crown dentin and 0.2 mm in root dentin with a CT scanning speed of 10.0 mm/s and a voxel size of 0.08 mm. The average of the three scanned slices was taken as the mineral density of the specimen.

The mineral densities of the specimens were compared among different age groups with under 30, 30–40, 40–50, and over 50 by analysis of variance (ANOVA) and Sheffe's *F*-test at a 95% level of confidence (STATVIEW 5.0, Abacus Concepts). The correlations between mineral density and age were analysed mathematically (Analysis ToolPak in Excel 2007, Microsoft).

1.1.3 Measurement of flexural strength and fracture toughness

Flexural fracture testing was conducted with beam-shaped specimens using the three-point bending geometry (Fig. 1D) with a universal testing machine (AUTOGRAPH AG-IS, Shimadzu). Samples were loaded to failure under moist conditions with HBSS at ambient temperature with a crosshead speed of 0.1 mm/min. Flexure strength (σ , N/mm²) was calculated with the following equation:

$$\sigma = 3PL/2wt^2$$

where P (N) is the maximum load at fracture, L (mm) is the support span (L = 2 mm, constant), and w (mm) and t (mm) are the width and thickness of the specimen, respectively. Fracture toughness (u , N/mm²) was also calculated from the stress-strain curve of the flexure testing with the following equation:

$$u = U (3/L)(y_{max}^2/I_x)$$

where U (N/mm) is the absorption energy to failure, L (mm) is the support span ($L = 2$ mm, constant), y_{max} (mm) is the distance of the surface from the neutral surface, and I_x (mm⁴) is the moment of inertia of the area given by:

$$y_{max} = t/2$$

$$I_x = wt^3/12.$$

The mechanical properties among individual specimens with different tubule orientations were compared by two-factor ANOVA followed by a Tukey's honestly significant difference (HSD) test at a 95% level of confidence (SPSS 18.0, IBM). Specimens of different age groups were compared by one-factor ANOVA and Sheffé's *F* test at a 95% level of confidence (STATVIEW 5.0, Abacus Concepts). The correlations between mechanical properties and age were analysed mathematically (Analysis ToolPak in Excel 2007, Microsoft).

1.1.4 Calculation of dentinal tubule density and degree of occluded tubule lumens

Fracture surfaces of the specimens in the transverse group were observed by scanning electron microscopy (SEM; JSM6390LV, JEOL) at a magnification of $\times 2,000$. Surfaces were sputter-coated with a gold-palladium alloy prior to observation. Dentinal tubule density was defined as the average numbers of dentinal tubules per unit area from five locations in the centre of the tensile side in the SEM images. The degree (%) of occluded tubule lumens was calculated as the number of perfectly occluded tubule lumens divided by the total number of dentinal tubules.

The correlations between the flexure strength and dentinal tubule density and degree of occluded tubule lumens were analysed mathematically (Analysis ToolPak in Excel 2007, Microsoft).

1.1.5 Measurement of hardness and Young's modulus

Semicircle-shaped specimens were polished by using emery waterproof abrasive papers (#1000, 1500, 2000, Sankyo-Rikagaku) and buffering cloths with alumina polishing suspension (1.0CR, 0.3CR, 0.05CR, Baikalox CR, Baikowski). The specimens were ultrasonically cleaned in deionized water for 5 min to remove the debris on their surfaces. The water temperature was kept below 37°C during the ultrasonic exposure to prevent deterioration of the mechanical properties of dentin. The dentin specimens were dried in air for 1 d at room temperature.

Nanoindentation was conducted by using a diamond Berkovich pyramidal indenter with a load-control-type nanoindentation system (ENT-1100a, ELIONIX). The maximum indentation load was 1 mN and the duration of the testing force was 180 s. The indentation was performed five times each for peritubular and intertubular dentin in a specimen while observing with a charge-coupled device microscope attached to the nanoindentation system.

1.2 Results

1.2.1 Mineral density

The mineral density of crown and root dentin was $1,479 \pm 45$ and $1,493 \pm 33$ mg/cm³, respectively. Both mineral densities increased with aging (Figs. 2 and 3). The mineral density of crown dentin taken from individuals younger than age 50 was significantly lower than that from individuals older than 50 ($p < 0.05$) (Fig. 2). The results also showed that the mineral density in crown dentin evidently increased more with aging than that in root dentin (Fig. 3).

1.2.2 Flexure strength and fracture toughness

Flexural strength of crown dentin in the anti-plane longitudinal, in-plane longitudinal, and transverse groups was 210 ± 67 , 193 ± 65 and 114 ± 36 MPa, respectively, and that of root dentin was 282 ± 105 MPa. Transverse specimens presented significantly lower fracture strength compared to those in other groups ($p < 0.01$, Fig. 4). In all the tested groups, the flexure strength decreased with aging (Fig. 5). From the statistical comparison among all kinds of specimens classified according to their age groups, overall, the age 40 was considered as the boundary of the flexure strength of human dentin (Fig. 6). Therefore, in further analyses, we compared the group with age over 40 to the group younger than age 40. The group with age over 40 showed significantly lower flexure strength than the younger group ($p < 0.05$) (Fig. 7).

Toughness in the anti-plane longitudinal, in-plane longitudinal, transverse, and root groups was 4.9 ± 2.9 , 3.6 ± 2.2 , 1.3 ± 1.0 , and 8.2 ± 5.0 MPa, respectively. Toughness showed a tendency similar to that of flexure strength. The transverse group showed significantly lower toughness compared to other groups ($p < 0.01$) (Fig. 8). Toughness in all groups with different tubule orientations decreased with aging (Fig. 9). The group with age over 40 showed significantly lower toughness than the younger group, except for the transverse specimens ($p < 0.05$) (Fig. 10).

1.2.3 Dentinal tubule density and degree of occluded tubule lumens

Dentin with high dentinal tubule density tended to have low flexure strength (Fig. 11). Dentin with high mineral density presented low flexure strength, and this tendency seemed clearer in the group with age over 40 (Fig. 12A). The group with age under 40, which showed low mineral density, displayed low degree of occluded tubule lumens, while the aged group, which showed high mineral density and high degree of occluded tubule lumens, displayed low flexure strength (Fig. 12B). Figure 13 shows the SEM images

of typical fracture surfaces of young and aged dentin. Aged dentin with high degree of occluded tubule lumens resulting in higher mineral density showed lower flexure strength and toughness than the young dentin with low degree of occluded tubule lumens.

1.2.4 Hardness and Young's modulus

The hardness of intertubular dentin was 0.9 ± 0.1 GPa and that of peritubular dentin was 1.6 ± 0.3 GPa. The Young's moduli of intertubular dentin and peritubular dentin were 24.8 ± 1.6 and 34.9 ± 3.9 GPa, respectively. The hardness and the Young's modulus of both intertubular and peritubular dentin did not change with aging (Fig. 14).

1.3 Discussion

In total, 32 third molars and 14 first and second molars were selected for the present study. Even distributions of these molars to the analysing groups in terms of age, type of teeth, and reasons for extraction were difficult because most of the third molars were obtained from young patients (age under 40) due to pericoronitis, while the first and second molars were from aged patients with advanced periodontitis. In summary, it was difficult to obtain aged third molars or young first and second molars. Therefore, the mechanical properties presented in this study might be affected by the background characteristics of each individual patient.

The results showed that the flexure strength of the transverse group was significantly lower than that in the other groups (Fig. 4). Arola *et al.*²¹ previously investigated the effects of tubule orientation on flexure strength and reported that the flexure strength of anti-plane longitudinal and transverse groups was 160 ± 22 and 109 ± 10 MPa. In the present study, the flexure strength of these groups was 210 ± 67 and 114 ± 36 MPa, respectively (Fig. 4), thus showing a similar tendency to that reported by Arola and

colleagues. The difference between the data in these two studies may be due to the different geometries of the bending tests. In the anti-plane longitudinal groups, which presented high flexure strength, the collagen fibrils distributed in the planes perpendicular to the tubules could effectively resist to crack propagation to fracture. The present study showed low flexure strength of aged dentin in all the groups with different tubule orientations (Fig. 7). The post-yielding strain of all the specimens was markedly low in the stress-strain curve of the flexure testing, and this explained the brittleness of dentin specimens. Therefore, the toughness showed a tendency similar to the flexure strength. Flexure strength and toughness of the root dentin showed large standard deviations (Figs. 4 and 8), because the regulation of the tubule orientations of the root dentin was difficult due to the curved, uneven configurations of the dentinal tubules.

Although Arola *et al.*²¹⁾ reported that dentin with high dentinal tubule density showed low flexure strength, such distinct tendency was not clear in our study (Fig. 11). This difference may be due to the different locations and tubule orientations of the dentin specimens in the two studies. In a previous study²¹⁾, anti-plane longitudinal specimens were taken from the outer third, middle, and inner third coronal dentin. In these three locations, there are differences in not only the dentinal tubule density but also in the size of tubule lumens²¹⁾. In the present study, the dentinal tubule densities were measured on the fracture surfaces of the transverse specimens. They corresponded approximately to the mid-coronal region and the sizes of the tubule lumens were well regulated. Therefore, the comparison of the present data to those in the previous study did not seem to be reasonable because of the different characteristics of the dentin specimens.

The hardness and the Young's modulus of both intertubular and peritubular dentin did not change with aging in spite of the high mineral density and high degree of occluded tubule lumens in aged specimens. This can be explained with the fact that mineralization with aging is not

attributed to the mineralization of intertubular and peritubular dentin, but mostly to the occlusion of dentinal tubule lumens with calcified materials. The occlusion of dentinal tubule lumens did not affect the hardness and the Young's modulus at the nano-level, but perhaps would affect them at the micro-level.

Nanoindentation was performed under dry conditions in the present study, despite the wet state in the oral cavity, because the corresponding measuring method is more stable and simple. Kinney *et al.*³⁵⁾ previously compared the hardness and Young's modulus of young dentin between wet and dry conditions. The Young's modulus of young intertubular dentin in wet condition was lower than that in dry condition, even though that in peritubular dentin did not appreciably change. This may be because peritubular dentin with very low organic content may be less affected by drying. On the other hand, the higher Young's modulus of intertubular dentin under the dry condition can be explained with the contractions of collagen fibrils due to loss of water. If the present study would have been performed under the wet condition, the Young's modulus of intertubular dentin might have been lower than the one obtained. However, the different conditions would hardly influence the individual differences of dentin.

In a crack propagation test of human dentin³⁶⁾, which was performed *in situ* with a static three-point bending while observing with an environmental scanning electron microscope stage, the crack-growth resistance of young dentin (19–30 years of age) was higher by approximately 40% compared to aged dentin (40–70 years of age), although the fracture toughness of crack-initiation in both groups was similar. Mechanistically, unfilled tubules tend to initiate microcracks prior to the main crack penetrating the tubule and result in crack deflection and branching (Fig.15). Unfilled tubules in young dentin had significantly more numerous microcracked tubules in the crack wake compared to aged dentin, which had fewer microcracks formed at occluded tubules. The linkage of microcracks of unfilled tubules to the main crack tip can result in regions of uncracked

material, which can act as uncracked-ligament bridging. On the other hand, occluded tubules in aged dentin presented less microcracking. At an early stage, a crack propagates around the peritubular cuff and does not penetrate the tubules, while, at a later stage, a crack propagates with less deflection and penetrates into occluded tubules. Less microcracking in aged dentin would lead to less ductility and reduced uncracked-ligament bridge formation³⁶⁾; therefore, aged dentin represented low fracture resistance. In the present study, which demonstrated that dentin with high degree of occluded tubule lumens shows low flexure strength, the same mechanism of crack propagation can be considered to explain the lower fracture resistance of aged dentin. Other studies of a fatigue fracture testing also claimed a similar mechanism of microcracking and crack bridging for explaining the low fracture resistance of aged dentin¹¹⁾.

1.4 Conclusion

The flexure strength and toughness of dentin showed apparent anisotropy according to dentinal tubule orientations. The flexure strength and toughness of the transverse group (114 ± 36 and 1.3 ± 1.0 MPa, respectively) were significantly lower than those of anti-plane longitudinal (210 ± 67 and 4.9 ± 2.9 MPa), in-plane longitudinal (193 ± 65 and 3.6 ± 2.2 MPa), and root (282 ± 105 and 8.2 ± 5.0 MPa) groups. The flexure strength and toughness of aged dentin (age ≥ 40) in all groups with different tubule orientations were significantly lower than those of young dentin (age < 40).

The mineral density resulting from the occlusion of the dentinal tubule with calcified materials increased with aging. This can be explained by the unchanged Young's modulus of the intertubular and peritubular dentin with aging. Dentin with high mineral density due to occlusion of the dentinal tubules showed low flexure strength.

Chapter 2

Mechanical strength of human dentin in relation to individual differences in microstructures and its compositions at the molecular level

2.1 Materials and methods

2.1.1 Preparation of dentin specimens

Beam-shaped specimens of crown and root dentin after the fracture testing, which were stored in HBSS at 4°C, were subject to the following experiments. A longitudinal section in the bucco-lingual plane with a thickness of approximately 0.2 mm was also obtained from every tooth used in the fracture testing (Fig. 1C).

2.1.2 Analysis of apatite orientation

The beam-shaped specimens with all the kinds of tubule orientations were used for analysing the distribution of the preferential alignment of the *c*-axis of biological apatite by using a microbeam X-ray diffraction system equipped with a transmission optical system (R-AXIS BQ, Rigaku)^{37, 38}. Molybdenum-K α radiation was generated at 50 kV and 90 mA (4.5 kW). The incident beam was collimated into a 300- μ m circular spot by a double-pinhole metal collimator and radiated vertically onto the specimen. The X-ray diffraction data were recorded using an imaging plate (Fuji Film) for 300 s and the (002) and (310) reflections were identified in the X-ray profile. The diffraction data parallel and perpendicular to the long axis of the specimens were extracted (Fig. 16) and the integrated intensity ratio of the (002) diffraction peak to the (310) diffraction peak was calculated. The intensity ratio corresponds to the degree of preferential alignment of the *c*-axis of the apatite crystallites³⁹.

The integrated intensity ratios between the directions parallel and perpendicular to the long axis of the specimens were compared by paired *t*-test. The correlations between the flexure strength and integrated intensity ratios were analysed mathematically (Analysis ToolPak in Excel 2007, Microsoft).

2.1.3 Measurement of collagen/mineral ratio

The ratios of collagen/mineral of the dentin were examined by Fourier transform infrared (FTIR) spectra analysis. The longitudinal sections were polished by using emery waterproof abrasive papers (#1000, 1500, 2000, Sankyo-Rikagaku) and buffering cloths with alumina polishing suspension (1.0CR, 0.3CR, 0.05CR, Baikalox CR, Baikowski). The specimens were ultrasonically cleaned in deionized water for 5 min to remove the debris on the surfaces and dried in air at room temperature. The absorption spectra were obtained using a FTIR spectrometer (NICOLET6700, Thermo scientific) with spectral resolution of 8 cm^{-1} and 128 scans per spectrum. These measures were obtained from the crown region at 1 mm from the dentin-enamel junction beneath the cusp and the root region at 1 mm above the apical area (indicated by red circles in Fig. 1C). The $\nu_3\text{PO}_4$ peaks at 980–1200 cm^{-1} and amide I peaks at 1595–1720 cm^{-1} in the spectra were identified to quantify the collagen/mineral ratios.

The effect of aging on the collagen/mineral ratios was analysed mathematically (Analysis ToolPak in Excel 2007, Microsoft). The correlations between the collagen/mineral ratios and flexure strength were also examined.

2.1.4 Quantification of advanced glycation end-products (AGEs)

Beam-shaped dentin specimens after the fracture testing were pulverized in a liquid nitrogen-cooled freezer mill. The powder was

demineralized with 0.5 M ethylenediaminetetraacetic acid (EDTA) in 50 mM Tris buffer (pH 7.4) for 96 h at 4°C. The demineralized dentin residues were then sequentially suspended in potassium phosphate buffer (pH 7.6, ionic strength 0.15) and reduced at 37°C with non-radioactive sodium borohydride (NaBH₄). The reduced specimens were hydrolysed in 6 M hydrochloric acid at 110°C for 24 h. The resulting hydrolysates were then analysed for cross-links by using high-performance liquid chromatography (HPLC) (LC9, Shimadzu) equipped with a cation exchange column (Aa pack-Na, JASCO) linked to an on-line fluorescence flow monitor (RF10AXL, Shimadzu).

The amount of AGEs (pentosidine), which is one of cross-links produced by non-enzymatic glycation, was detected by natural fluorescence with excitation at 335 nm and emission at 385 nm. The quantity of the cross-links was expressed as ng quinine/mg of collagen.

The correlations between the amount of cross-links and flexure strength with aging were analysed mathematically (Analysis ToolPak in Excel 2007, Microsoft).

2.2 Results

2.2.1 Apatite orientation

Based on the X-ray diffraction data parallel and perpendicular to the long axis of the specimens, the integrated intensity ratios of the parallel direction in the in-plane longitudinal and root groups were significantly higher than those of the perpendicular direction, and that of the perpendicular direction in the transverse group was significantly higher than that of the parallel direction ($p < 0.01$) (Fig. 16). The integrated intensity ratio in the anti-plane longitudinal did not show significant differences between the parallel and perpendicular directions. This revealed that the preferential alignment of the σ axis of apatite was perpendicular to the dentinal tubule orientation. The flexure strength significantly increased

in the specimens with strong alignment of their apatite c axis ($p < 0.05$) (Fig. 17).

2.2.2 Collagen/mineral ratio

The results from the FTIR microspectroscopy showed that the ratios of amide I peaks to $\nu_3\text{PO}_4$ peaks in both crown and root dentin varied in the range from 0.13 to 0.37, and both did not correlate with aging (Fig. 18A). The flexure strength neither showed a relation with the collagen/mineral ratios (Fig. 18B). This suggests that the ratio of collagen/mineral does not affect the mechanical properties of dentin.

2.2.3 AGEs content

The pentosidine content in crown dentin significantly increased with aging ($p < 0.05$), while that in root dentin did not increase significantly ($p = 0.22$) (Fig. 19A). The results also showed significant negative correlation between the flexure strength and the pentosidine content of both crown and root dentin ($p < 0.05$) (Fig. 19B).

2.3 Discussion

In the present study, the apatite crystal of dentin was proved to align perpendicular to the dentinal tubules (Fig. 19). Since the apatite in the cortical bone aligns parallel to the orientation of collagen fibrils^{40–42}, the apatite may align along the felt-like structure of collagen fibrils perpendicular to the tubule orientation. Strong alignment of dentin apatite may contribute to the anisotropy of the flexure strength of dentin according to the tubule orientation, since the apatite aligned along the collagen fibrils can reinforce the intertubular dentin resulting in increased fracture resistance. The anisotropy of dentin and cortical bone in relation to their

tubule structures was found to be different. Since the Haversian canals, which are microstructures in the cortical bone, align parallel to collagen fibrils in long bones, the Young's modulus of the long bone was high in the direction parallel to the Haversian canals⁴³⁻⁴⁶⁾.

The relative collagen/mineral ratio did not show any correlation with age nor with flexure strength (Fig. 17). Ager *et al.*⁴⁷⁾ reported on the strong amide I peak in aged demineralized and dehydrated dentin by using UV resonance Raman spectra analysis. Ryou *et al.*⁴⁸⁾ investigated the flexure strength of crown dentin taken from different locations in relation to mineral/collagen ratio, and indicated that deep dentin exhibited lower flexure strength than superficial dentin because the mineral/collagen ratio in deep dentin was approximately 20% higher than that in superficial dentin. However, as described in other reports^{21, 22)}, the differences in the mechanical properties of dentin taken from different locations were primarily attributed to the dentinal tubule density and tubule diameter. Pashley *et al.*⁴⁹⁾ also correlated the decrease in dentin microhardness from the dentin-enamel junction towards the pulp with the increase in tubule density, and such low hardness in the deep dentin was considered to be mainly due to the large tubule diameter and the lower amount of intertubular dentin. A similar correlation was also found in other studies investigating the tensile strength²²⁾ and root dentin⁵⁰⁾. Various results from these reports indicated that the mechanical strength of dentin should be evaluated by comprehensively including its microstructures and compositions.

Collagen cross-links can be divided into lysyl hydroxylase and lysyl oxidase-mediated enzymatic immature divalent cross-links, mature trivalent pyridinoline and pyrrole cross-links, and AGEs induced by non-enzymatic glycation or oxidation reaction such as glucosepane and pentosidine⁵¹⁻⁵⁵⁾. Recently, collagen enzymatic and non-enzymatic cross-links in bone have been proved to affect not only the mineralization process but also microdamage. Saito *et al.*^{56, 57)} examined the BMD and the content of enzymatic and non-enzymatic cross-links of cortical bone in sound and

osteoporosis patients with femoral neck fracture. The results suggested that the low levels of BMD and enzymatic collagen cross-links as well as excessive formation of pentosidine might cause the low bone strength in osteoporosis patients^{58–66}). Based on these findings, the quality and quantity of collagen cross-links have been widely accepted as a significant factor regulating the mechanical properties of bone^{51, 61, 67–69}). Furthermore, serum or urine pentosidine levels are now being used to estimate future fracture risk in osteoporosis and diabetes^{70–74}). Miura *et al.*³⁰ confirmed by immunohistochemical analysis that CML, which is an AGEs, accumulated in the collagen fibrils around the dentinal tubules in aged dentin. In the present study, aged dentin with high level of pentosidine content was proved to have low flexure strength (Fig. 19). Aged dentin collagen becomes more fragile because of the accumulated AGEs. This can be considered as one of the reasons for the lower mechanical strength of aged dentin.

2.4 Conclusion

The preferential alignment of the *c*-axis of apatite was proved to be perpendicular to the dentinal tubule orientation. The degree of its alignment may contribute to the anisotropy of the flexure strength of dentin, because the apatite aligned along the collagen fibrils can reinforce the intertubular dentin resulting in increased fracture resistance.

The pentosidine content in crown dentin significantly increased with aging. Aged dentin collagen becomes more fragile because of the accumulated AGEs, and this may be one of the reasons for the lower flexural strength of aged dentin.

Chapter 3

Dominant factors to mechanical strength of human dentin

3.1 Materials and methods

A multiple linear regression (MLR) analysis was performed to identify the dominant factors that affect the mechanical strength of dentin by using the analytical software JMP-10 (SAS). In this study, stepwise regression and least squares regression were used. Flexure strength was identified as an objective variable, while explanatory variables were age, mineral density, number of dentinal tubules, degree of occluded tubule lumens, pentosidine content and apatite orientation. In the stepwise regression, a regression model was built by iteratively including or eliminating items from a list of explanatory variables. All factors with p -values less than 0.05 were used to generate the stepwise linear regression model. The least corrected Akaike information criterion (AICc) was used for presenting the statistically significant combination of parameters for predicting the objective variable. Furthermore, least squares regression was conducted to identify the influential explanatory variables to the objective variable from the views of quality and structural parameters separately, where the quality parameters were mineral density, apatite orientation and pentosidine content, while the structural parameters were degree of occluded tubule lumens and number of dentinal tubules. The variance inflation factor (VIF) was also considered to qualify the severity of multicollinearity in the least squares regression analysis.

3.2 Results

The complete data sets of all the analysed factors from 14 teeth were used for the MLR analysis. The data of flexure strength were selected as the objective variable. The results indicated that age was the significant

parameter demonstrating the least AICc (Table 1). Since age was identified as the most influential factor to regulate the flexure strength of dentin, further analysis was performed to clarify which factors were significant to explain the aging of dentin. In the least squares regression analysis pertaining to the quality parameters, the pentosidine content and mineral density were identified as influential factors (Table 2A). This regression model can be considered statistically significant ($R^2 = 0.76$, $p < 0.01$). The analysis of the structural parameters demonstrated that the degree of occluded tubule lumens was an influential factor (Table 2B). However, the result of this regression did not seem to be powerful ($R^2 = 0.16$, $p = 0.10$).

3.3 Discussion

The VIF indexes of both quality and structural parameter groups were below 1.5 (Table 2), indicating that the analysis was not affected by the multicollinearity.

The least squares regression analysis presented that both mineral density and pentosidine content were important factors to account for the mechanical strength of dentin, as those have been well acknowledged as influential factors for regulating bone strength. Although the crack propagation in dentin was influenced by the occluded tubules, the distinct influence of occluded tubules to the flexure strength was not proved by the statistical analysis. Additional specimens would be required to detect a much clearer significance of occluded tubules.

3.4 Conclusion

A multiple linear regression analysis indicated that the high mineral density due to occlusion of dentinal tubules and accumulation of AGEs in dentin collagen with aging were significant factors that caused the low mechanical strength of aged dentin.

GENERAL CONCLUSIONS

Flexure strength and toughness of human dentin decrease with aging. High mineral density due to occlusion of dentinal tubule and accumulation of AGEs in dentin collagen were identified as the primary causes for the low mechanical strength of aged dentin.

REFERENCES

- 1) Nanci A (2003). Dentin-pulp complex. In Nanci A (Ed.), *Ten Cate's oral histology: Development, structure, and function* (pp.192-215). Missouri: Mosby.
- 2) Zaslansky P (2008). Dentin. In Fratzl P (Ed.), *Collagen: Structure and mechanics* (pp. 421-446). New York: Springer.
- 3) Pashley DH (1989). Dentin: A dynamic substrate-a review. *Scanning Microsc* 3:161-176.
- 4) Marshall Jr GW, Marshall SJ, Kinney JH, Balooch M (1997). The dentin substrate: structure and properties related to bonding. *J Dent* 25:441-458.
- 5) Arola D, Reprogl R (2005). Effects of aging on the mechanical behavior of human dentin. *Biomaterials* 26:4051-4061.
- 6) Vasiliadis L, Darling AI, Levers BG (1983). The amount and distribution of sclerotic human root dentine. *Arch Oral Biol* 28:645-649.
- 7) Natusch I, Pilz ME, Klimm W, Buchmann G (1989). Transparent dentinal sclerosis and its clinical significance. *Zahn Mund Kieferheikd Zentralbl* 77:3-7.
- 8) Vasiliadis L, Darling AI, Levers BG (1983). The histology of sclerotic human root dentine. *Arch Oral Biol* 28:693-700.
- 9) Micheletti CM (1998). Dental histology: study of aging processes in root dentine. *Boll Soc Ital Biol Sper* 74:19-28.

10) Weber DF (1974). Human dentin sclerosis: a microradiographic survey. *Arch Oral Biol* 19:163-169.

11) Kinney JH, Nalla RK, Pople JA, Breunig TM, Ritchie RO (2005). Age-related transparent root dentin: mineral concentration, crystallite size, and mechanical properties. *Biomaterials* 26:3363-3376.

12) Giachetti L, Ercolani E, Bambi C, Landi D (2002). Sclerotic dentin: aetiopathogenetic hypothesis. *Minerva Stomatol* 51:285-292.

13) van Huysen G (1960). The microstructure of normal and sclerosed dentine. *J Prosthet Dent* 10:976-982.

14) Balooch M, Demos SG, Kinney JH, Marshall GW, Balooch G, Marshall SJ (2001). Local mechanical and optical properties of normal and transparent root dentin. *J Mat Sci Mater Med* 12:507-514.

15) Porter AE, Nalla RK, Minor A, Jinscheck JR, Kisielowski C, Radmilovic V, Kinney JH, Tomsia AP, Ritchie RO (2005). A transmission electron microscopy study of mineralization in age-induced transparent dentin. *Biomaterials* 26:7650-7660.

16) Toto PD, Kastelic EF, Duyvejonck KJ, Rapp GW (1971). Effect of age on water content in human teeth. *J Dent Res* 50:1284-1285.

17) Tagami J, Hosoda H, Burrow MF, Nakajima M (1992). Effect of aging and caries on dentin permeability. *Proc Finn Dent Soc* 88:149-154.

18) Jameson MW, Hood JA, Tidmarsh BG (1993). The effects of dehydration and rehydration on some mechanical properties of human dentine. *J Biomech* 26:1055-1065.

19) Kahler B, Swain MW, Moule A (2003). Fracture-toughening mechanisms responsible for differences in work of fracture of hydrated and dehydrated dentin. *J Biomech* 36:229-237.

20) Bajaj D, Sundaram N, Nazari A, Arola D (2006). Age, dehydration and fatigue crack growth in dentin. *Biomaterials* 27:2507-17.

21) Arola D, Reprogl R (2006). Tubule orientation and fatigue strength of human dentin. *Biomaterials* 27:2131-2140.

22) Inoue S, Pereira PN, Kawamoto C, Nakajima M, Koshiro K, Tagami J, Carvalho RM, Pashley DH, Sano H (2003). Effect of depth and tubule direction on ultimate tensile strength of human coronal dentin. *Dent Mater J* 22:39-47.

23) Carvalho RM, Fernandes CA, Villanueva R, Wang L, Pashley DH (2001). Tensile strength of human dentin as a function of tubule orientation and density. *J Adhes Dent* 3:309-314.

24) Lertchirakarn V, Palamara JE, Messer HH (2001). Anisotropy of tensile strength of human dentin. *J Dent Res* 80:453-456.

25) Bedran-de-Castro AK, Perreira PN, Thompsom JY (2004). Influence of load cycling and tubule orientation on ultimate tensile strength of dentin. *J Adhes Dent* 6:191-194.

26) Nalla RK, Kinney JH, Ritchie RO (2003). Effect of orientation on the in vitro fracture toughness of dentin: the role of toughening mechanisms. *Biomaterials* 24:3955-3968.

27) Arola D, Rouland J (2003). The effects of tubule orientation on fatigue crack growth in dentin. *J Biomed Mater Res* 67:78-86.

28) Miguez PA, Pereira PN, Atsawasuwa P, Yamauchi M (2004). Collagen cross-linking and ultimate tensile strength in dentin. *J Dent Res* 83:807-810.

29) Açil Y, Springer IN, Prasse JG, Hedderich J (2002). Concentration of collagen cross-links in human dentin bears no relation to the individual age. *Int J Legal Med* 116:340-343.

30) Miura J, Nishikawa K, Kubo M, Fukushima S, Hashimoto M, Takeshige F, Araki T (2014). Accumulation of advanced glycation end-products in human dentine. *Arch Oral Biol* 59:119-124.

31) World Health Organization (1994). Assessment of fracture risk and its application to screening for postmenopausal osteoporosis. Report of a WHO Study Group. *WHO Tech Rep Ser* 843:1-129.

32) NIH Consensus Development Panel on Osteoporosis Prevention, Diagnosis, and Therapy (2001). Osteoporosis prevention, diagnosis and therapy. *JAMA* 285:785-795.

33) 中野貴由 (2007). 結晶工学的手法による骨質評価と結晶配向に基づくバイオマテリアルの設計. *バイオマテリアル—生体材料*—25:112-122.

34) Turner CH, Burr DB (1993). Basic biomechanical measurements of bone: a tutorial. *Bone* 14:595-608.

35) Kinney JH, Habelitz S, Marshall SJ, Marshall GW (2003). The importance of intrafibrillar mineralization of collagen on the mechanical properties of dentin. *J Dent Res* 82:957-961.

36) Koester KJ, Ager JW 3rd, Ritchie RO (2008). The effect of aging on crack-growth resistance and toughening mechanisms in human dentin. *Biomaterials* 29:1318-1328.

37) Sasaki K, Nakano T, Ferrara JD, Lee LW, Sasaki T (2008). New technique for evaluation of preferential alignment of biological apatite (BAp) crystallites in bone using transmission X-ray diffractometry. *Mater Trans* 49:2129-2135.

38) Noyama Y, Nakano T, Ishimoto T, Sakai T, Yoshikawa H (2013). Design and optimization of the oriented groove on the hip implant surface to promote bone microstructure integrity. *Bone* 52:659-667.

39) Nakano T, Kaibara K, Tabata Y, Nagata N, Enomoto S, Marukawa E, Umakoshi Y (2002). Unique alignment and texture of biological apatite crystallites in typical calcified tissues analyzed by microbeam X-ray diffractometer system. *Bone* 31:479-487.

40) Robinson RA, Watson ML (1952). Collagen-crystal relationships in bone as seen in the electron microscope. *Anat Rec* 114:383-410.

41) Arsenault AL (1988). Crystal-collagen relationships in calcified turkey leg tendons visualized by selected-area dark field electron microscopy. *Calcif Tissue Int* 43:202-212.

42) Kikuchi M, Itoh S, Ichinose S, Shinomiya K, Tanaka J (2001). Self-organization mechanism in a bone-like hydroxyapatite/collagen nanocomposite synthesized in vitro and its biological reaction in vivo. *Biomaterials* 22:1705-1711.

43) Bonfield W, Grynpas MD (1977). Anisotropy of the Young's modulus of bone. *Nature* 270:453-454.

44) Sasaki N, Matsushima N, Yamamura H, Fukuda AJ (1989). Orientation of bone mineral and its role in the anisotropic mechanical properties of bone-transverse anisotropy. *J Biomech* 22:157-164.

45) Sasaki N, Sudoh Y (1997). X-ray pole figure analysis of apatite crystals and collagen molecules in bone. *Calcif Tissue Int* 60:361-367.

46) Ziv V, Wagner HD, Weiner S (1996). Microstructure-microhardness relations in parallel-fibered and lamellar bone. *Bone* 18:417-428.

47) Ager JW 3rd, Nalla RK, Balooch G, Kim G, Pugach M, Habelitz S, Marshall GW, Kinney JH, Ritchie RO (2006). On the increasing fragility of human teeth with age: a deep-UV resonance raman study. *J Bone Miner Res* 21:1879-1887.

48) Ryou H, Amin N, Ross A, Eidelman N, Wang DH, Romberg E, Arola D (2011). Contributions of microstructure and chemical composition to the mechanical properties of dentin. *J Mater Sci: Mater Med* 22:1127-1135.

49) Pashley D, Okabe A, Parham P (1985). The relationship between dentin microhardness and tubule density. *Endod Dent Traumatol* 1:176-179.

50) Mannocci F, Pilecki P, Bertelli E, Watson TF (2004). Density of dentinal tubules affects the tensile strength of root dentin. *Dent Mater* 20:293-296.

51) Vashishth D, Gibson GJ, Khouri JI, Schaffler MB, Kimura J, Fyhrie DP (2001). Influence of nonenzymatic glycation on biomechanical properties of cortical bone. *Bone* 28:195-201.

52) Paul RG, Bailey AJ (1996). Glycation of collagen: the basis of its central role in the late complications of ageing and diabetes. *Int J Biochem Cell Biol* 28:1297-1310.

53) Sell DR, Monnier VM (1989). Structure elucidation of a senescence cross-link from human extracellular matrix. Implication of pentoses in the aging process. *J Biol Chem* 264:21597-21602.

54) Uchiyama A, Ohishi T, Takahashi M, Kushida K, Inoue T, Fujie M, Horiuchi K (1991). Fluorophores from aging human articular cartilage. *J Biochem* 110:714-718.

55) Brownlee M (1994). Lilly Lecture 1993. Glycation and diabetic complications. *Diabetes* 43:836-841.

56) Saito M, Fujii K, Soshi S, Tanaka T (2006). Reductions in degree of mineralization and enzymatic collagen cross-links and increases in glycation-induced pentosidine in the femoral neck cortex in cases of femoral neck fracture. *Osteoporos Int* 17:986-995.

57) Saito M, Fujii K, Marumo K (2006). Degree of mineralization-related collagen crosslinking in the femoral neck cancellous bone in cases of hip fracture and controls. *Calcif Tissue Int* 79:160-168.

58) Vashishth D (2007). The role of the collagen matrix in skeletal fragility. *Curr Osteoporos Rep* 5:62-66.

59) Hernandez CJ, Tang SY, Baumbach BM, Hwu PB, Sakkee AN, van der Ham F, DeGroot J, Bank RA, Keaveny TM (2005). Trabecular microfracture and the influence of pyridinium and non-enzymatic glycation-mediated collagen cross-links. *Bone* 37:825-832.

60) Viguet-Carrin S, Farlay D, Bala Y, Munoz F, Bouxsein ML, Delmas PD (2008). An in vitro model to test the contribution of advanced glycation end products to bone biomechanical properties. *Bone* 42:139-149.

61) Wang X, Shen X, Li X, Agrawal CM (2002). Age-related changes in the collagen network and toughness of bone. *Bone* 31:1-7.

62) Saito M, Fujii K, Mori Y, Marumo K (2006). Role of collagen enzymatic and glycation induced cross-links as a determinant of bone quality in spontaneously diabetic WBN/Kob rats. *Osteoporos Int* 17:1514-1523.

63) Garnero P, Borel O, Gineyts E, Duboeuf F, Solberg H, Bouxsein ML, Christiansen C, Delmas PD (2006). Extracellular post-translational modifications of collagen are major determinants of biomechanical properties of fetal bovine cortical bone. *Bone* 38:300-309.

64) Saito M, Mori S, Mashiba T, Komatsubara S, Marumo K (2008). Collagen maturity, glycation induced-pentosidine, and mineralization are increased following 3-year treatment with incadronate in dogs. *Osteoporos Int* 19:1343-1354.

65) Silva MJ, Brodt MD, Lynch MA, McKenzie JA, Tanouye KM, Nyman JS, Wang X (2009). Type 1 diabetes in young rats leads to progressive trabecular bone loss, cessation of cortical bone growth, and diminished whole bone strength and fatigue life. *J Bone Miner Res* 94:1618-1627.

66) Viguet-Carrin S, Roux JP, Arlot ME, Merabet Z, Leeming DJ, Byrjalsen I, Delmas PD, Bouxsein ML (2006). Contribution of the advanced glycation end product pentosidine and of maturation of type I collagen to compressive biomechanical properties of human lumbar vertebrae. *Bone* 39:1073-1079.

67) Oxlund H, Mosekilde L, Ortoft G (1996). Reduced concentration of collagen reducible cross links in human trabecular bone with respect to age and osteoporosis. *Bone* 19:479-484.

68) Oxlund H, Barckman M, Ortoft G, Andreassen TT (1995). Reduced concentrations of collagen cross-links are associated with reduced strength of bone. *Bone* 17:365S-371S.

69) Ziopoulos P, Currey JD, Hamer AJ (1999). The role of collagen in the declining mechanical properties of aging human cortical bone. *J Biomed Mater Res* 45:108-116.

70) Saito M, Marumo K (2010). Collagen cross-links as a determinant of bone quality: a possible explanation for bone fragility in aging, osteoporosis, and diabetes mellitus. *Osteoporos Int* 21:195-214.

71) Shiraki M, Urano T, Kuroda T, Saito M, Tanaka S, Miyao-Koshizuka M, Inoue S (2008). The synergistic effect of bone mineral density and methylenetetrahydrofolate reductase (MTHFR) polymorphism (C677T) on fractures. *J Bone Miner Metab* 26:595-602.

72) Shiraki M, Kuroda T, Tanaka S, Saito M, Fukunaga M, Nakamura T (2008). Nonenzymatic collagen cross-links induced by glycoxidation (pentosidine) predicts vertebral fractures. *J Bone Miner Metab* 26:93-100.

73) Shiraki M, Kuroda T, Shiraki Y, Tanaka S, Higuchi T, Saito M (2011). Urinary pentosidine and plasma homocysteine levels at baseline predict future fractures in osteoporosis patients under bisphosphonate treatment. *J Bone Miner Metab* 29:62-70.

Explanatory variables included in the regression model	AICc
age	147
age, pentosidine content	150
age, number of dentinal tubules, pentosidine content	151
age, number of dentinal tubules, degree of occluded tubule lumens, pentosidine content	153
age, mineral density, number of dentinal tubules, degree of occluded tubule lumens, pentosidine content	161
age, mineral density, number of dentinal tubules, degree of occluded tubule lumens, pentosidine content, apatite orientation	172

Table 1 Stepwise regression for the identification of the dominant factors influencing the flexure strength

A Quality parameters

	estimated coefficient	standard error	t-values	p-values	standard partial regression coefficient	variance inflation factor
intercept	1839.20	340.75	5.40	0.0003	0	—
mineral density	-0.89	0.22	-3.99	0.0026	-0.63	1.02
apatite orientation	103.78	73.20	1.42	0.1867	0.26	1.44
pentosidine content	-1.66	0.40	-4.10	0.0022	-0.76	1.42

($R^2 = 0.76, p < 0.01$)

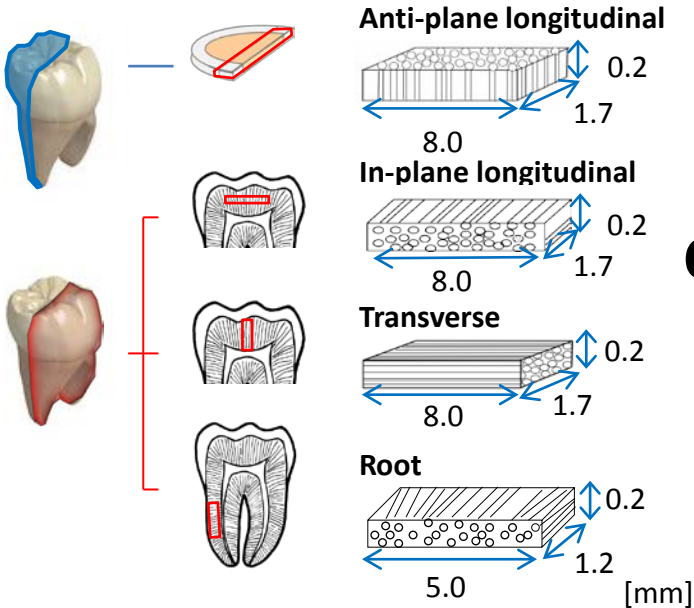
B Structural parameters

	estimated coefficient	standard error	t-value	p-value	standard partial regression coefficient	variance inflation factor
intercept	239.10	65.69	3.64	0.0011	0	—
degree of occluded tubule lumens	-1.27	0.57	-2.23	0.0340	-0.41	1.06
number of dentinal tubules	-0.31	0.62	-0.49	0.6259	-0.09	1.06

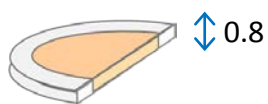
($R^2 = 0.16, p = 0.10$)

Table 2 Least squares regression for the analysis of the parameters explaining the influence of aging

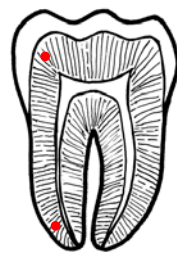
A Beam-shaped specimen



B Semicircle-shaped specimen



C Longitudinal thin section



D

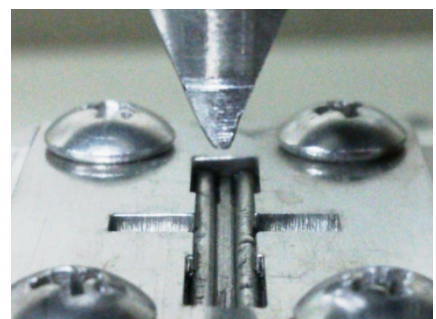
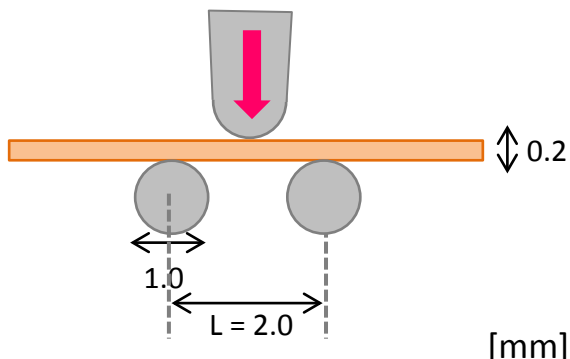
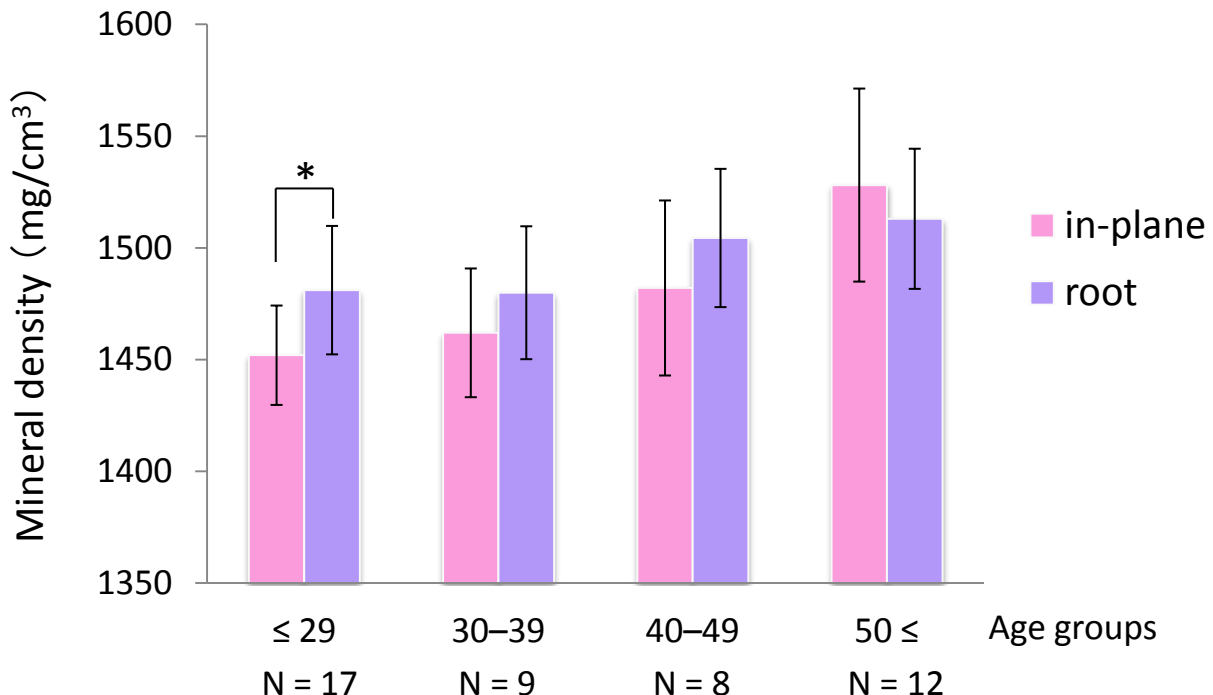


Fig. 1 Configurations of human dentin specimens and geometry of the flexural fracture testing

Beam-shaped specimens of crown dentin with three different dentinal tubule orientations and root dentin (A), a semicircle -shaped specimen (B), and a longitudinal 0.2-mm thin section (C) were obtained from one tooth. The red circles in the thin section represent the locations where the Fourier transform infrared (FTIR) spectra were quantified. Specimens subjected to flexural fracture testing were secured as a three-point bending geometry (D).



*: Statistically significant difference calculated by paired *t*-test ($p < 0.01$).

Statistical analysis by one-factor ANOVA and Sheffe's *F*-test ($p < 0.05$)

Types of specimens	Age groups			
	≤ 29	30–39	40–49	$50 \leq$
in-plane	a	a	a	b
root	a	a	a	a

a,b, : No statistically significant differences between the groups indicated by the same letters.

ANOVA: Analysis of variance

Fig. 2 Mineral density of human dentin in different age groups.

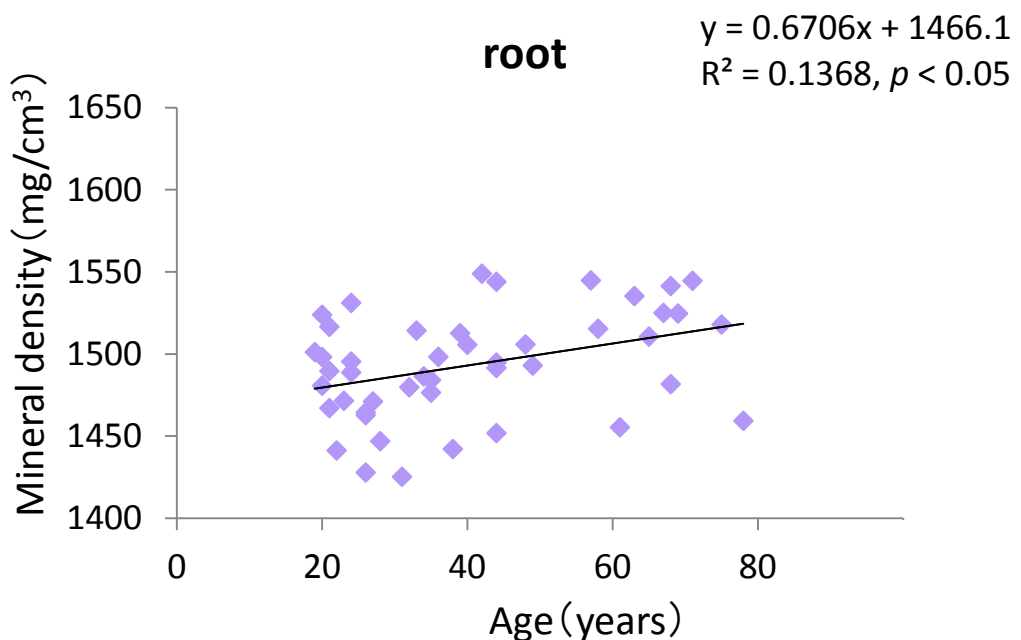
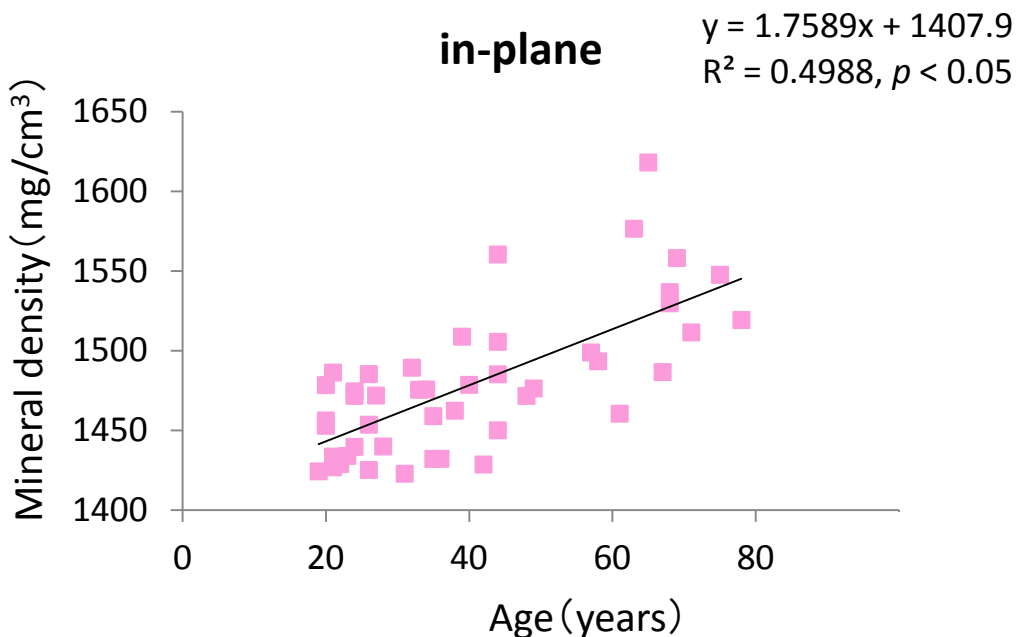


Fig. 3 Mineral density of crown and root dentin taken from individuals with ages from 19 to 78 years.

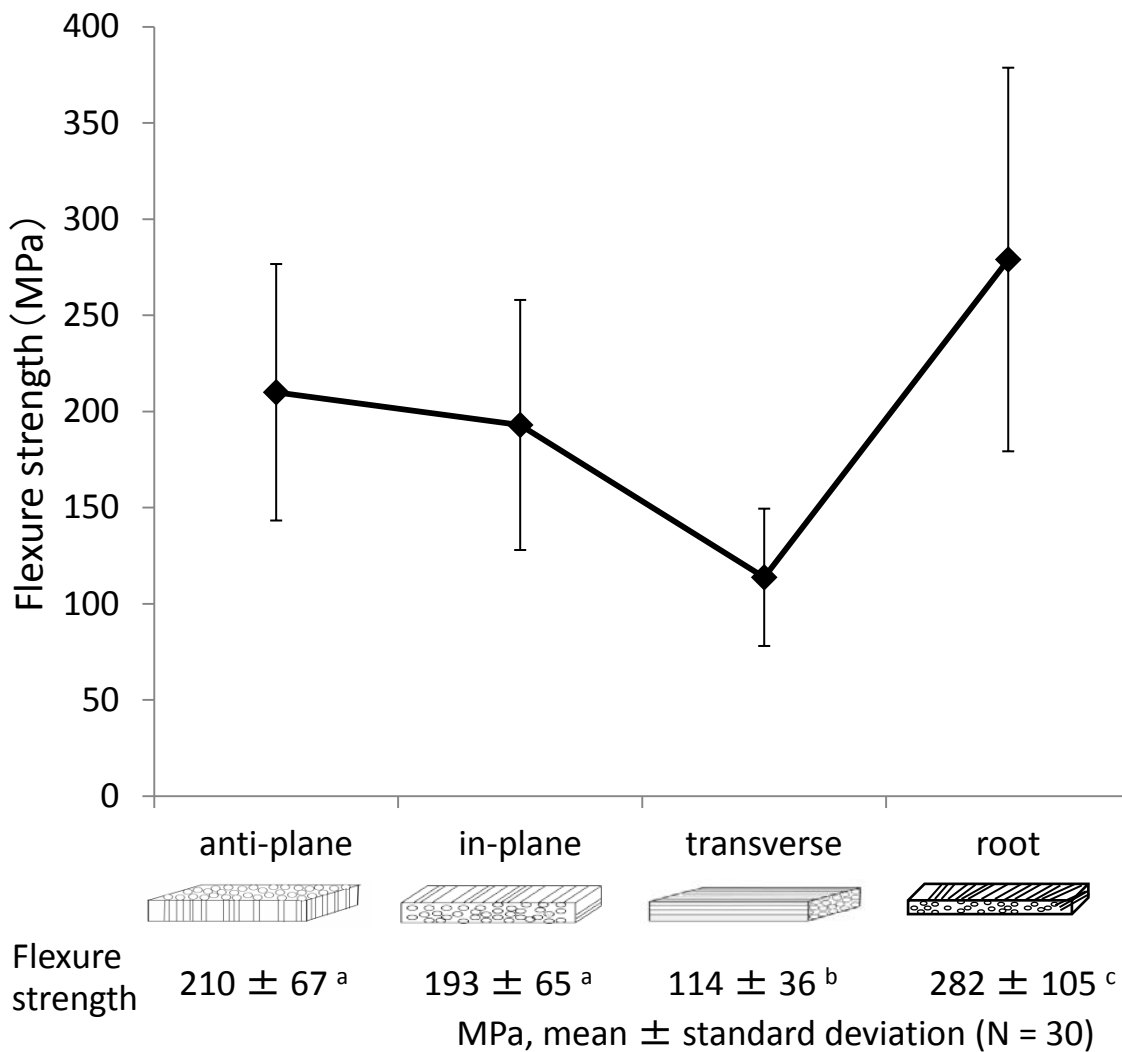


Fig. 4 Flexure strength of human crown and root dentin with different tubule orientations.

a,b,c : No statistically significant differences between the groups indicated by the same letters (two-factor ANOVA, Tukey's HSD test, $p < 0.01$). ANOVA: analysis of variance; HSD: honestly significant difference.

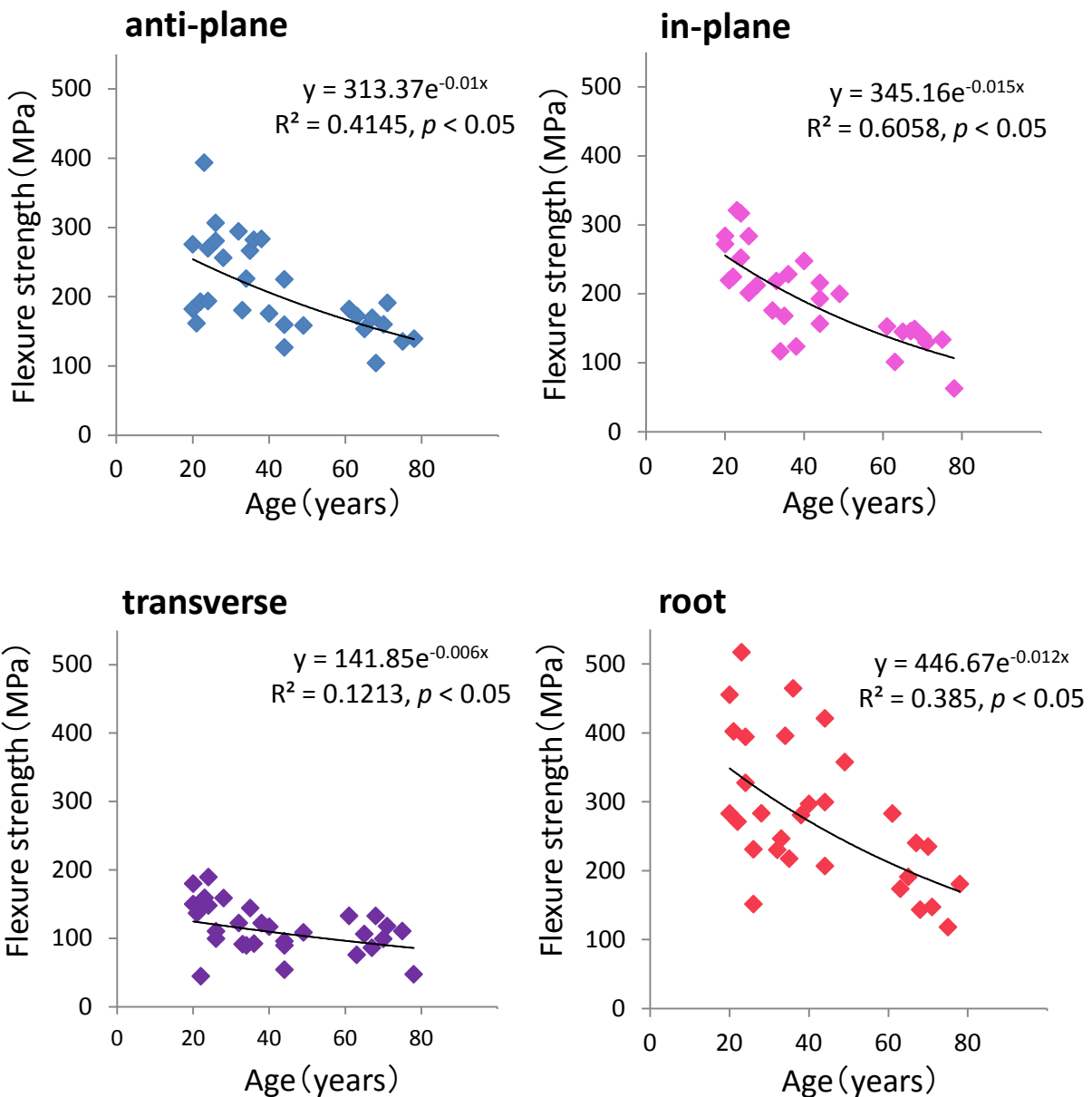
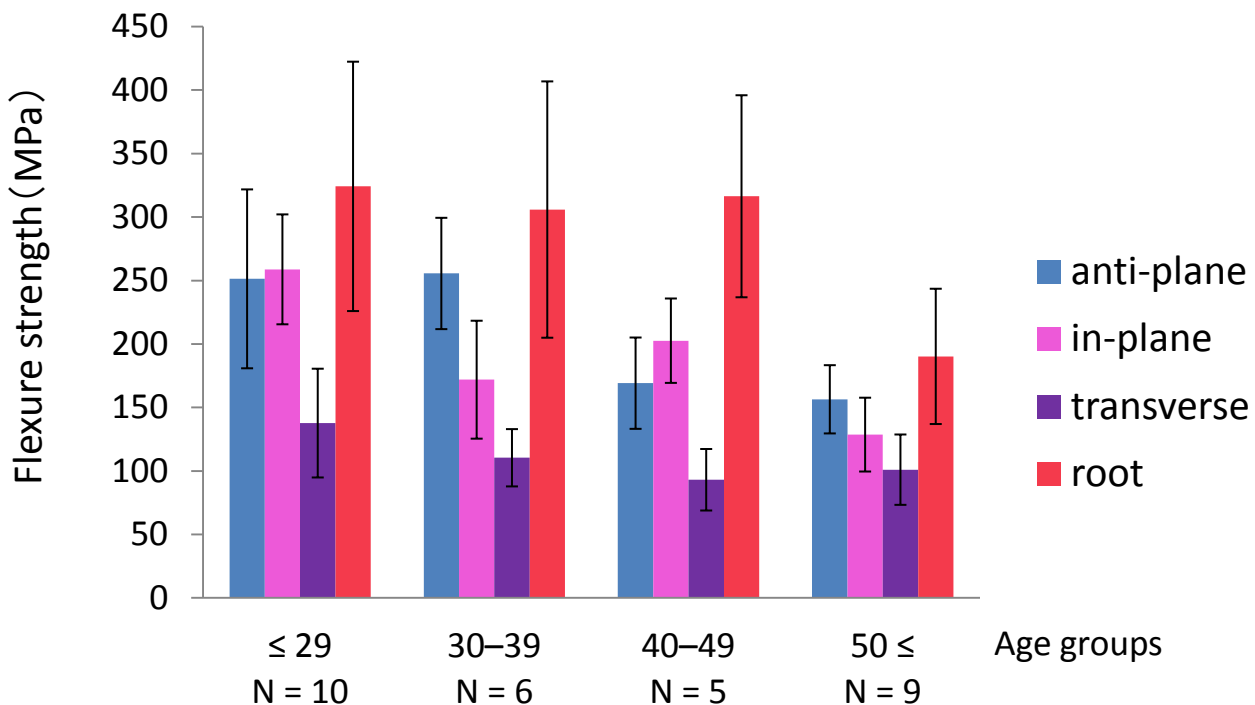


Fig. 5 Correlation between age and flexure strength of human crown and root dentin with different tubule orientations.



Statistical analysis by one-factor ANOVA and Sheffe's F-test ($p < 0.05$)

Types of specimens	Age groups	≤ 29	30–39	40–49	50 ≤
anti-plane		a	ac	bc	b
in-plane		a	bc	ac	b
transverse		a	a	a	a
root		a	a	a	a

a,b,c : No statistically significant differences between the groups indicated by the same letters. ANOVA: Analysis of variance

Fig. 6 Flexure strength of human dentin with three dentinal tubule orientations in different age groups.

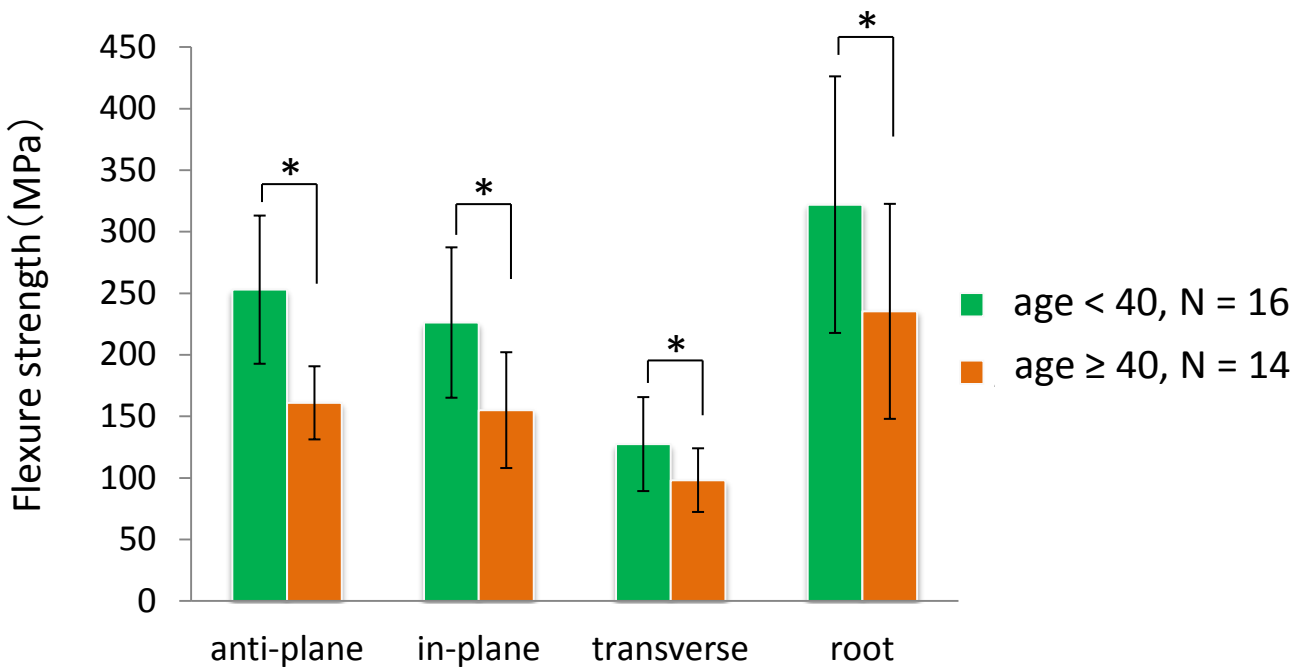


Fig. 7 Flexure strength of human crown and root dentin with different tubule orientations in the aged (age ≥ 40) and the young (age < 40) groups.

*: Statistically significant differences between the aged and young groups (t -test, $p < 0.05$).

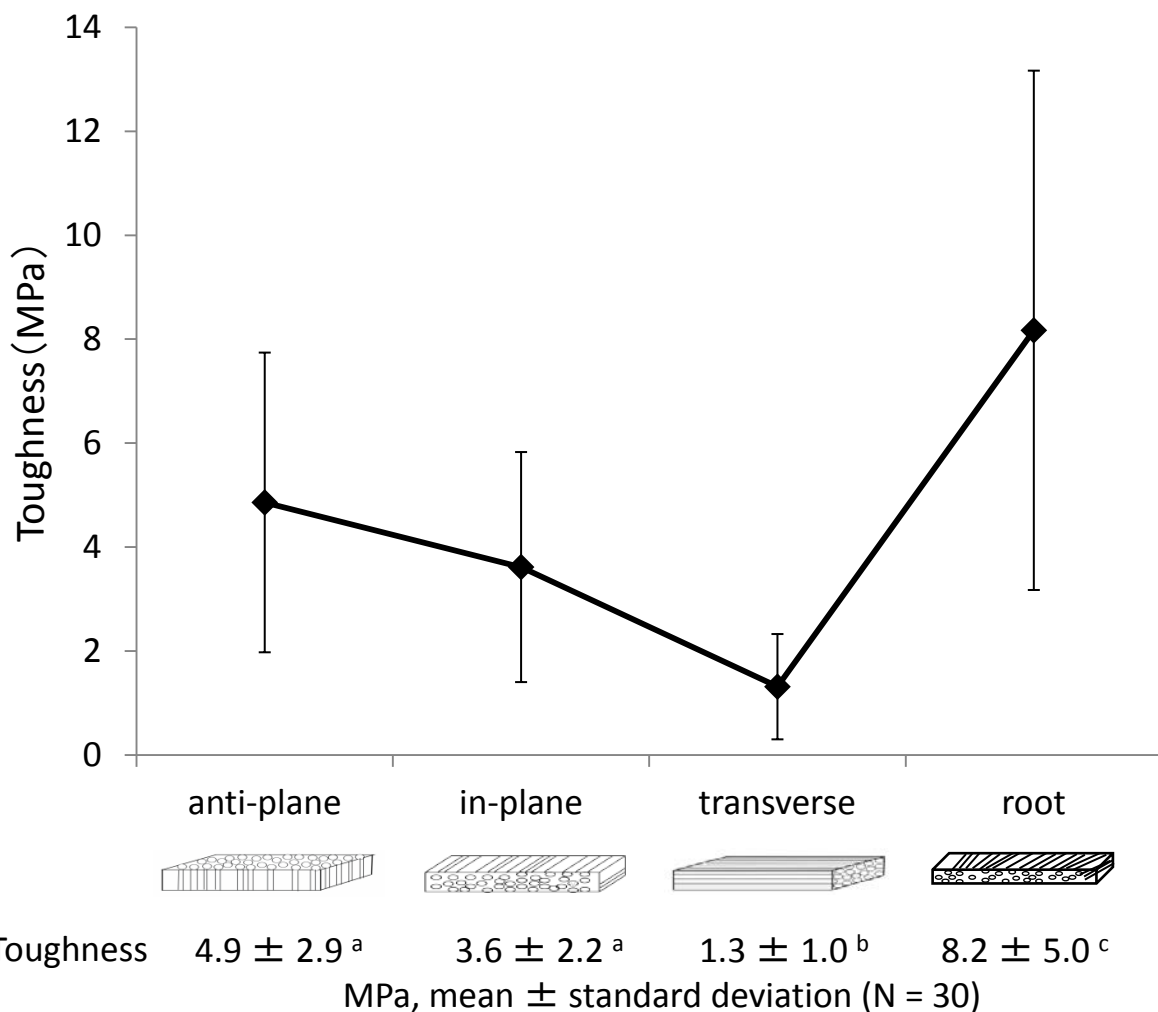


Fig. 8 Toughness of human crown and root dentin with different tubule orientations.

a,b,c : No statistically significant differences between the groups indicated by the same letters (two-factor ANOVA, Tukey's HSD test, $p < 0.01$). ANOVA: analysis of variance; HSD: honestly significant difference.

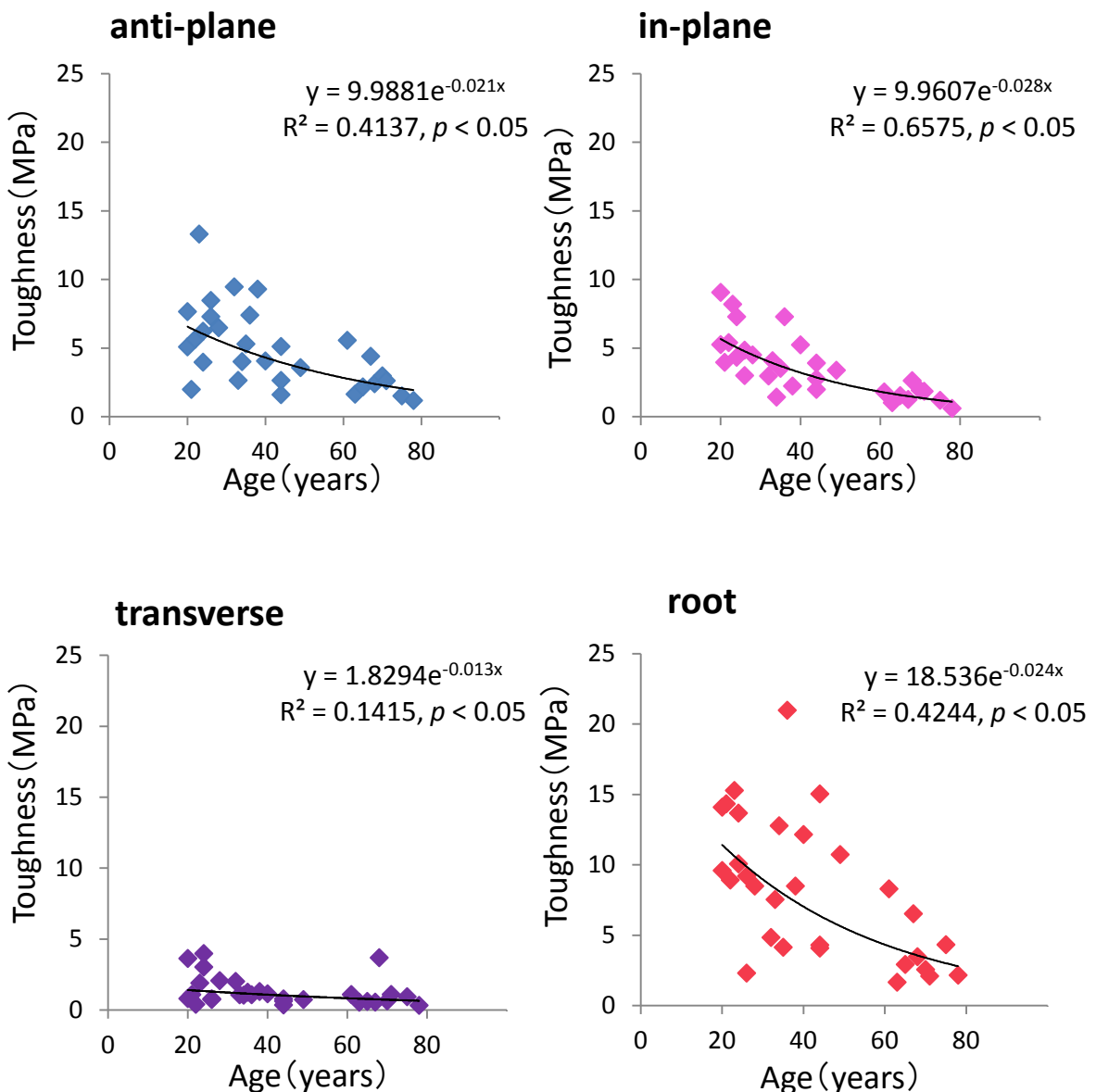


Fig. 9 Correlation between age and toughness of human crown and root dentin with different tubule orientations.

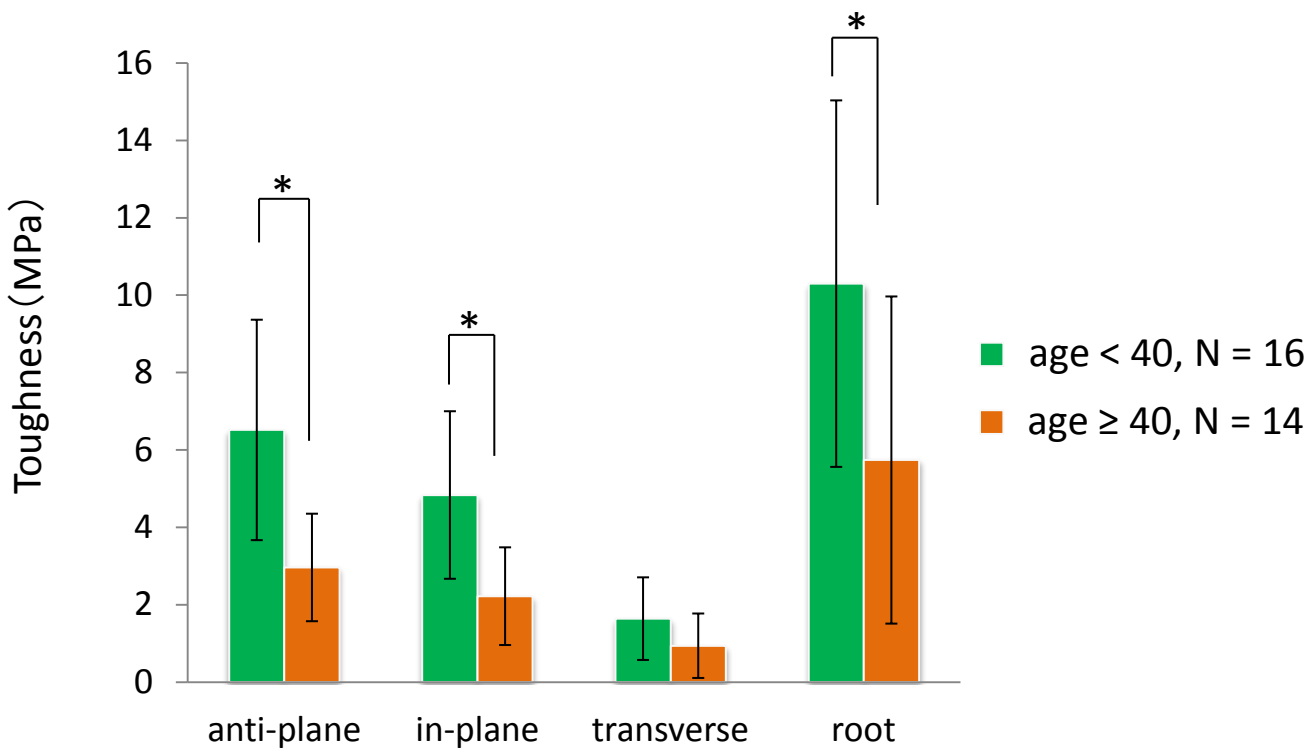


Fig. 10 Toughness of human dentin with different tubule orientations in the aged (age ≥ 40) and the young (age < 40) groups.

*: Statistically significant differences between the aged and young groups (t -test, $p < 0.05$).

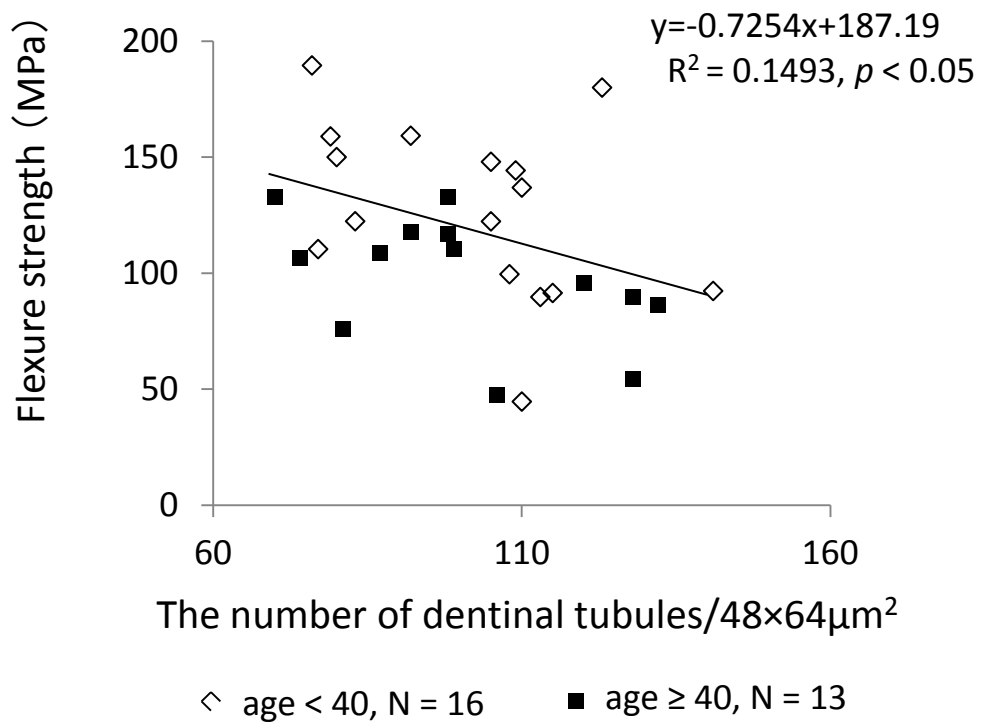
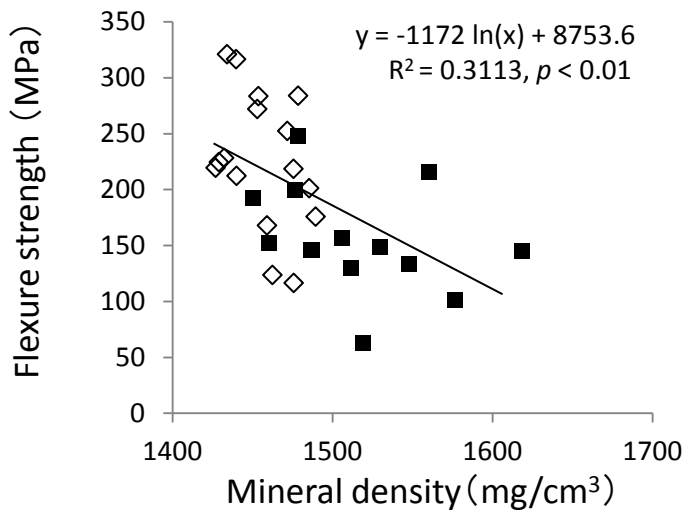
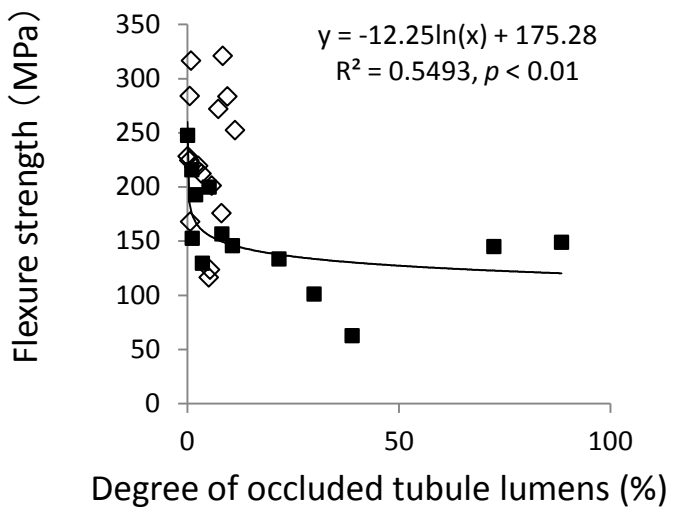
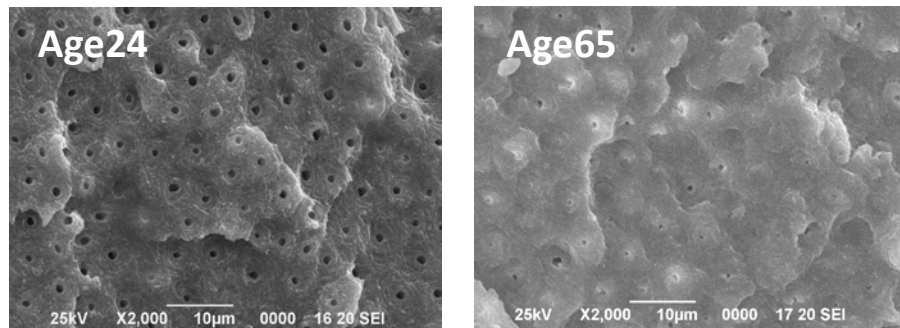


Fig. 11 Effect of dentinal tubule density on the flexure strength of human crown dentin in transverse group.

A**B**

◇ age < 40, N = 16 ■ age ≥ 40 , N = 13

Fig. 12 Effects of mineral density (A) and degree of occluded tubule lumens (B) on flexure strength of human crown dentin in in-plane longitudinal group.



	Age 24	Age 65
Mineral density (mg/cm ³)	1471	1618
Flexure strength transverse (MPa)	148	106
Flexure strength in-plane (MPa)	252	145

Fig. 13 Scanning electron microscopy (SEM) images of fracture surfaces of young and aged human dentin in relation with their physical properties.

Aged dentin with occluded tubule lumen showed higher mineral density and lower flexure strength than young dentin with open tubule lumen.

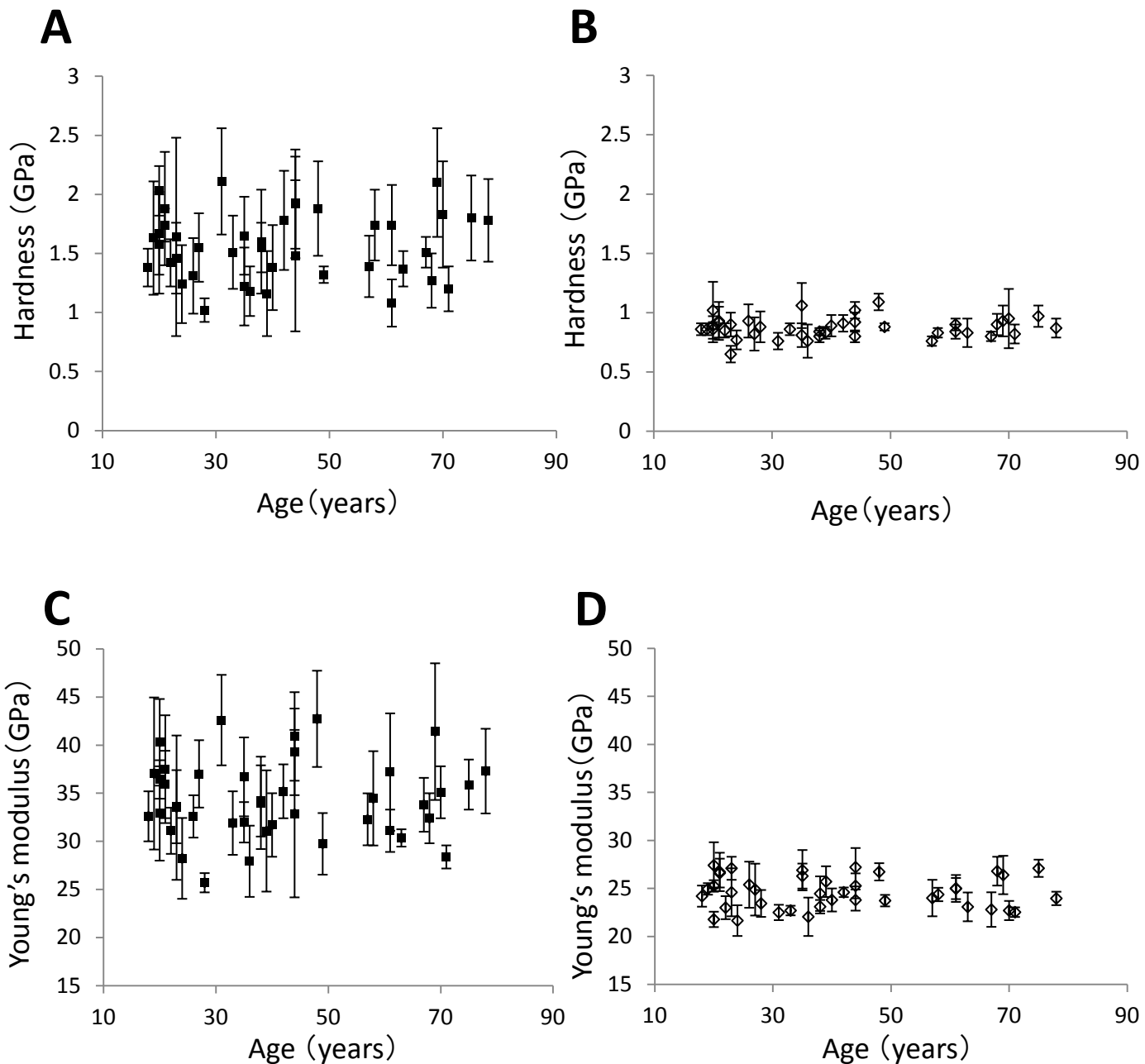
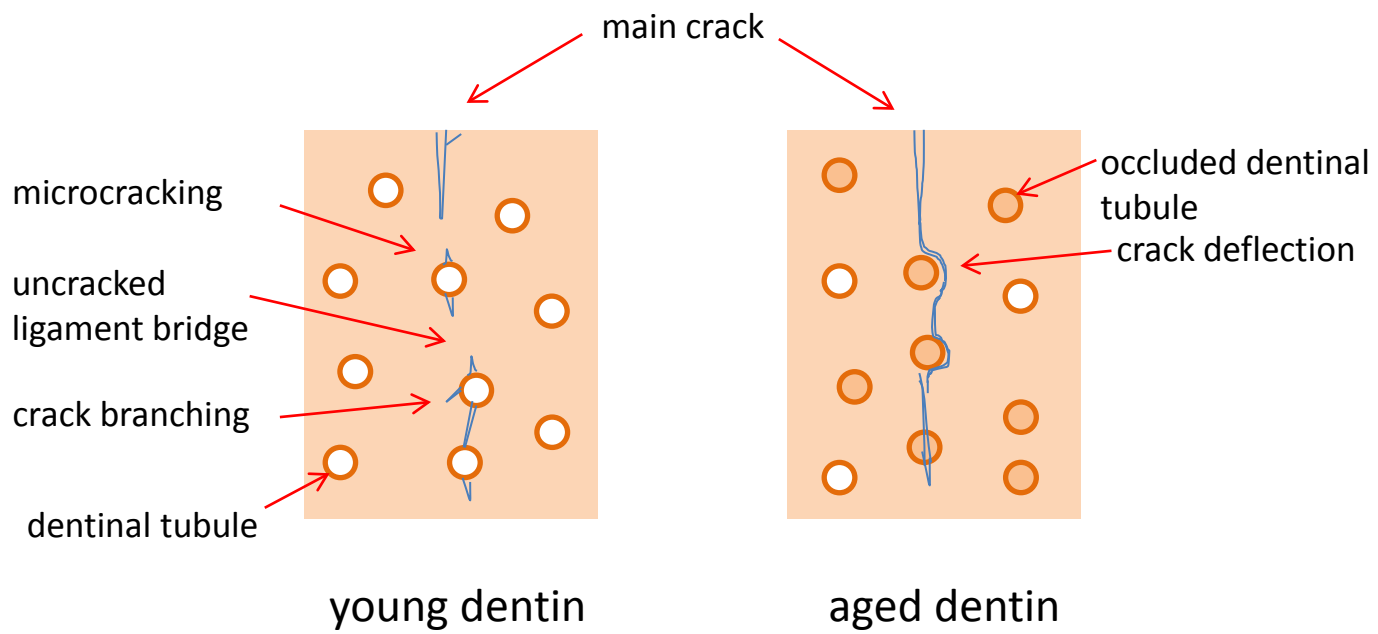


Fig. 14 Hardness and Young's modulus of human crown dentin taken from individuals with ages from 18 to 78 years.

A and C: peritubular dentin; B and D: intertubular dentin.



(Koester *et al.*, Biomaterials 2008)

Fig. 15 Schematic diagrams of crack propagation in human dentin.

Integrated intensity ratio of (002)/(310) corresponding to the preferential alignment of the *c*-axis of apatite

Types of specimen	anti-plane	in-plane	transverse	root
Measuring direction				
Parallel	1.1 \pm 0.1	1.3 \pm 0.1*	0.8 \pm 0.1	1.3 \pm 0.4*
Perpendicular	1.3 \pm 0.2	0.8 \pm 0.1	1.2 \pm 0.1*	0.9 \pm 0.2
mean \pm standard deviation (N = 25)				

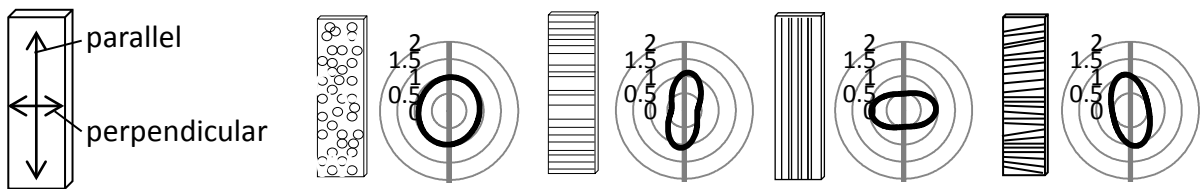


Fig. 16 Distribution of the *c*-axis of apatite in human crown and root dentin with different tubule orientations.

*: Statistically significant differences between parallel and perpendicular directions (paired *t*-test, $p < 0.01$).

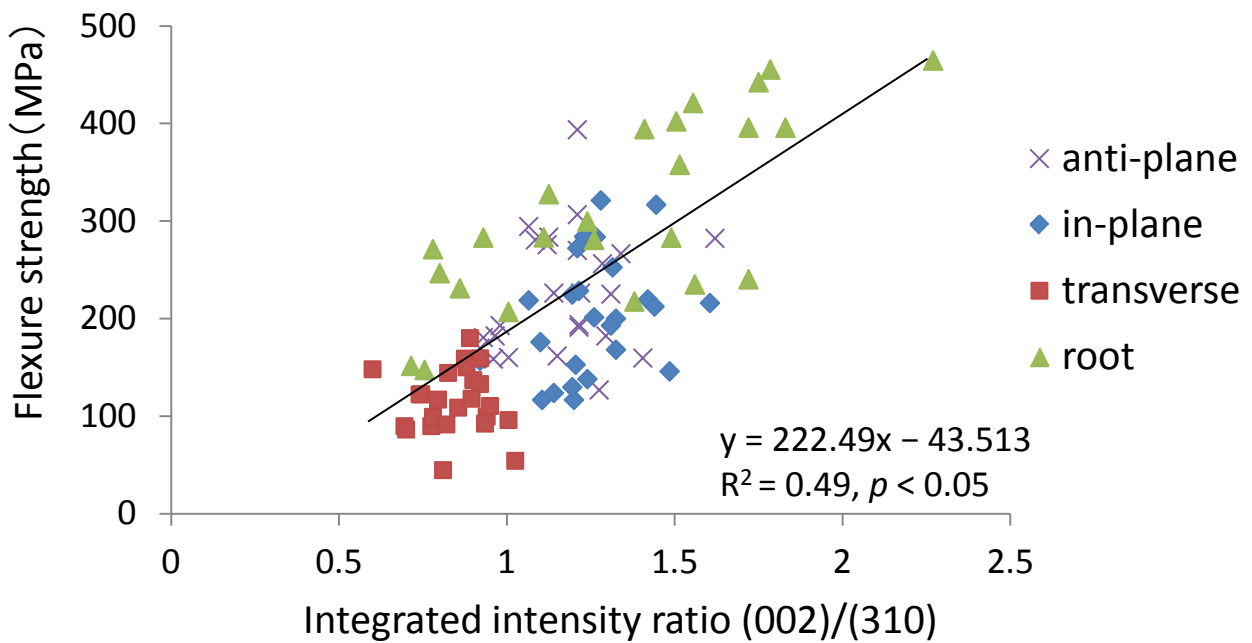


Fig. 17 Effects of the apatite orientations on the flexure strength of human crown and root dentin.

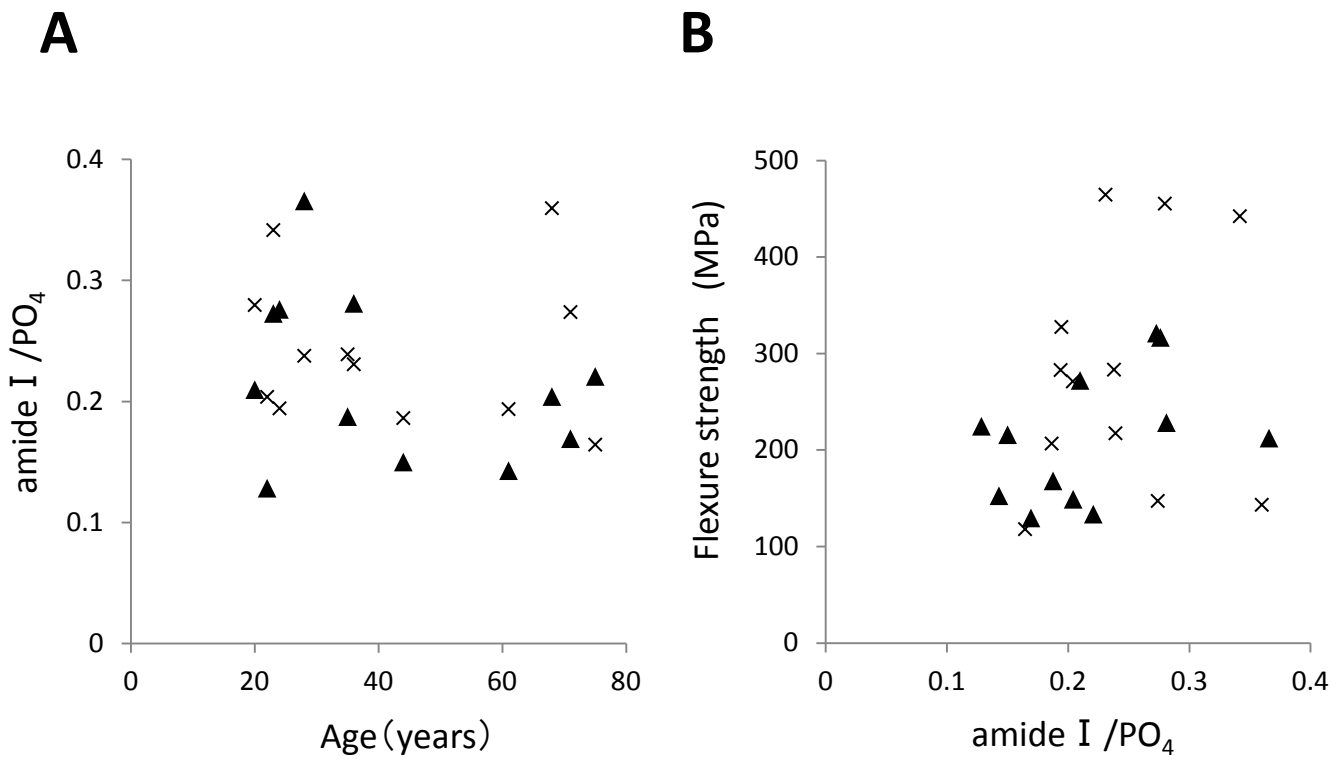


Fig. 18 Collagen/mineral ratios of human dentin in relation to aging (A) and flexure strength (B).
 (▲: crown dentin, ×: root dentin)

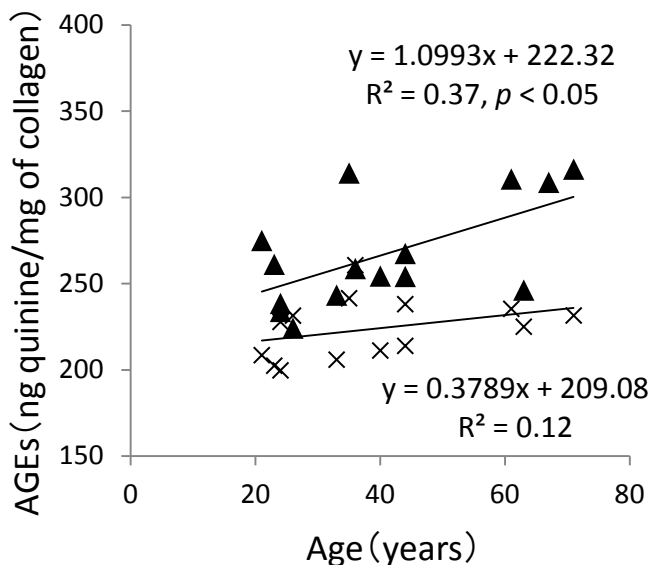
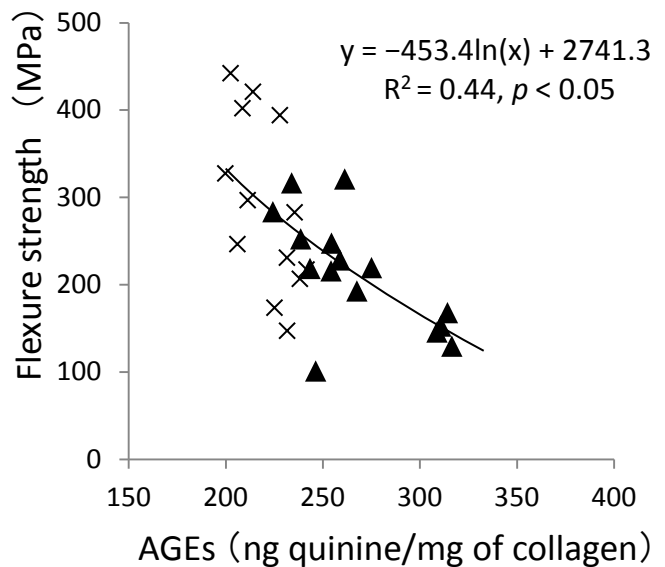
A**B**

Fig. 19 Quantity of advanced glycation end-products (AGEs; i.e., pentosidine) in human dentin collagen in relation with aging (A) and flexure strength (B).
(▲: crown dentin, ×: root dentin)